THE FASEB JOURNAL • RESEARCH • www.fasebj.org

Genome-wide screening identifies novel genes and biological processes implicated in cisplatin resistance

Tengyu Ko and Shisheng Li[1]
Department of Comparative Biomedical Sciences, School of Veterinary Medicine, Louisiana State University, Baton Rouge, Louisiana, USA

ABSTRACT: Cisplatin-based chemotherapeutic regimens are frequently used for treatments of solid tumors. However, tumor cells may have inherent or acquired cisplatin resistance, and the underlying mechanisms are largely unknown. We performed genome-wide screening of genes implicated in cisplatin resistance in A375 human melanoma cells. A substantial fraction of genes whose disruptions cause cisplatin sensitivity or resistance overlap with those whose disruptions lead to increased or decreased cell growth, respectively. Protein translation, mitochondrial respiratory chain complex assembly, signal recognition particle–dependent cotranslational protein targeting to membrane, and mRNA catabolic processes are the top biologic processes responsible for cisplatin sensitivity. In contrast, proteasome-mediated ubiquitin-dependent protein catabolic process, negative regulations of cellular catabolic process, and regulation of cellular protein localization are the top biologic processes responsible for cisplatin resistance. ZNRF3, a ubiquitin ligase known to be a target and negative feedback regulator of Wnt–β-catenin signaling, enhances cisplatin resistance in normal and melanoma cells independently of β-catenin. Ariadne-1 homolog (ARIH1), another ubiquitin ligase, also enhances cisplatin resistance in normal and melanoma cells. By regulating ARIH1, neurofibromin 2, a tumor suppressor, enhances cisplatin resistance in melanoma but not normal cells. Our results shed new lights on cisplatin resistance mechanisms and may be useful for development of cisplatin-related treatment strategies.—Ko, T., Li, S. Genome-wide screening identifies novel genes and biological processes implicated in cisplatin resistance. FASEB J. 33, 7143–7154 (2019). www.fasebj.org

KEY WORDS: CRISPR-Cas9 · ZNRF3 · NF2 · ARIH1

Cisplatin-based chemotherapeutic regimens are the most frequently used adjuvant or neoadjuvant treatments for the majority of solid tumors. After its *cis*-chloro groups are replaced by water molecules, cisplatin forms covalent bonds with methionine and a large panel of cysteine-containing peptides and polypeptides and reacts with DNA to produce intra- and interstrand crosslinks (1). Cisplatin treatment is highly efficient against testicular germ cell cancer, leading to a durable complete remission in >80% of patients (2). However, clinical responses elicited by cisplatin-based therapeutic regimens in patients affected by other solid tumors are temporary and vanish as malignant cells become chemoresistant.

Cisplatin resistance is complex and may be caused by different mechanisms, including *1*) decreased drug intake or increased drug extrusion by plasma membrane transporters, *2*) increased nuclear and mitochondrial DNA repair and preservation or turnover of cytoplasmic components, *3*) altered checkpoints and safeguard mechanisms, and *4*) molecular circuitries that deliver compensatory survival signals even though they are not directly activated by cisplatin (1, 3). However, despites decades of intensive effort, the genes and biologic processes implicated in cisplatin resistance are still largely unknown.

Melanoma is the most aggressive skin cancer and notoriously resistant to chemotherapeutic agents, including cisplatin (4). Marked improvements in melanoma treatments, especially those with small-molecule targeted drugs and immunotherapies, have been achieved over the past decade. However, because of its high heterogeneity and high genetic mutation rate, metastatic melanoma is still one of the toughest cancers to treat. Insights into the mechanisms of cisplatin resistance will be useful for

ABBREVIATIONS: ARIH1, ariadne-1 homolog; Cas9, CRISPR-associated protein 9; CRISPR, clustered regularly interspaced short palindromic repeat; CTNNB1, catenin β-1; FDR, false discovery rate; EIF4E2, eukaryotic translation initiation factor 4E 2; GAPDH, glyceraldehyde-3-phosphate dehydrogenase; GeCKO, Genome-Scale CRISPR Knock-Out; GO, gene ontology; LRP5/6, LDL receptor–related proteins 5 and 6; MAGeCK, model-based analysis of genome-wide CRISPR-Cas9 knockout; NF2, neurofibromin 2; P1F/TERT, TERT immortalized human fibroblast; RNF7, ring finger protein 7; RNF43, ring finger protein 43; RPMI, Roswell Park Memorial Institute; sgRNA, single-guide RNA; shRNA, small hairpin RNA; shZNRF3, ZNRF3-targeting shRNA; TEAD, transcriptional enhancer associated domain; TERT, telomerase; TRC, the RNA Interference Consortium; UBE2F, ubiquitin-conjugating enzyme E2 F; VISPR, visualization of CRISPR screens; YAP, yes-associated protein; ZNRF3, zinc and ring finger 3

[1] Correspondence: Department of Comparative Biomedical Sciences, School of Veterinary Medicine, Louisiana State University, 1909 Skip Bertman Dr., Baton Rouge, LA 70803, USA. E-mail: shli@lsu.edu

doi: 10.1096/fj.201801534RR
This article includes supplemental data. Please visit *http://www.fasebj.org* to obtain this information.

development of novel treatment strategies for melanoma as well as other types of cancers.

Here, we report the identifications of genes and biologic processes implicated in cisplatin resistance by utilizing a genome-wide clustered regularly interspaced short palindromic repeat (CRISPR)–CRISPR-associated protein 9 (Cas9) gene knockout system. Interestingly, a large fraction of these genes and biologic processes have not been previously recognized as the leading causes of cisplatin resistance.

MATERIALS AND METHODS

Cell lines

A375 human melanoma cells were from American Type Culture Collection (Manassas, VA, USA; ATCC CRL-1619) and cultured in Roswell Park Memorial Institute (RPMI) 1640–GlutaMax medium supplemented with 10% of newborn calf serum. Human Hermes 4C melanocytes, which were immortalized by vectors expressing human telomerase (TERT) and human papillomavirus type 16, protein E7 (5, 6), were obtained from Wellcome Trust Functional Genomics Cell Bank (St. George's, University of London, London, United Kingdom) and cultured in RPMI 1640–GlutaMax medium supplemented with 10% newborn calf serum, human stem cell factor (10 ng/ml), phorbal-12-myristate-13-acetate (200 nM), chlorotoxin (200 pM), and endothelin (10 nM). TERT immortalized human fibroblast (P1F/TERT) was obtained from the Rheinwald Laboratory (Harvard Skin Disease Research Center, Harvard Medical School, Boston, MA, USA) and cultured in DMEM-F12 medium supplemented with 15% newborn calf serum and 10 ng/ml of epidermal growth factor.

Genome-scale CRISPR knockout library preparation and lentivirus production

Genome-scale CRISPR Knock-Out (GeCKO) libraries (1000000048; Addgene, Watertown, MA, USA) were transformed into Endura electrocompetent *Escherichia coli* cells (60242; Lucigen, Middleton, WI, USA). To ensure adequate coverage of the single-guide RNAs (sgRNAs) contained in the libraries, $>10^8$ independent *E. coli* transformants were obtained. After overnight culturing in lysogeny broth medium, plasmids were purified by using a Plasmid Maxi Kit (Qiagen, Germantown, MD, USA). To prepare lentiviral particles expressing Cas9 and the GeCKO library sgRNAs, the plasmids were cotransfected with plasmids pCMV-VSV-G (8454; Addgene) and psPAX2 (12260; Addgene) into human embryonic kidney 293T cells (632180; Clontech Laboratories, Mountain View, CA, USA) (7). Lentiviral particles were harvested 48 h after the transfection, concentrated by ultracentrifugation at 24,000 rpm for 2 h at 4°C, and resuspended in RPMI 1640 medium containing 10% fetus bovine serum by incubation at 4°C overnight.

GeCKO library transduction and cisplatin treatment of A375 human melanoma cells

The protocol is outlined in **Fig. 1*A***. One hundred million melanoma A375 cells were transduced with lentiviral GeCKO libraries by using Spinfection (8), giving rise to a transduction efficiency of ~70–80%. Puromycin was added to the culture to a final concentration of 1 μg/ml 2 d after the transduction to eliminate untransduced cells. On d 7, cells were pooled, and one-third of the total population was harvested as early transduction (for estimation of distribution of transduced sgRNAs). The remaining cells were seeded back and cultured. On d 12, one-half of the cultured cells were treated with 8 μM cisplatin for 16 h, which killed ~50–60% of the cells, and the other half of the cells were left untreated. The cisplatin-treated and untreated cells were passaged synchronously to ensure they underwent similar numbers of cell divisions before harvesting. To maintain the coverage of the GeCKO libraries, the cells were pooled, and $>5 \times 10^7$ cells were seeded for each passage. Cisplatin-treated and untreated cells were harvested on d 25.

Next-generation sequencing of GeCKO sgRNAs

The genomic DNA was purified from the early transduction, and cisplatin-treated and untreated cells by using Blood and Cell Culture DNA Midi Kit (13343; Qiagen). sgRNA sequences were amplified by 18 cycles of PCR using 130 μg of the genomic DNA as templates (10 μg genomic DNA per PCR reaction), Lenti-F1 and Lenti-R1 primers (Supplemental Table S1), and Herculase II Fusion DNA polymerase (Agilent Technologies, Santa Clara, CA, USA). All PCR products of 400–600 bp in the same treatment group were combined and gel purified. Sequencing adapters (Illumina, San Diego, CA, USA) were attached to the purified DNA fragments by 24 cycles of PCR using GECKO1 and GECKO2-2 primers (Supplemental Table S1). Finally, barcode sequences were attached to the fragments by 12 cycles of PCR using Tru-U as forward and Tru-B1/2/3 as reverse primers (Supplemental Table S1). Sequencing was carried out on an Illumina Hi-Seq 2000 platform, and the data were analyzed by using model-based analysis of genome-wide CRISPR-Cas9 knockout (MAGeCK) and visualization of CRISPR screens (VISPR) (9), which allow for enrichment analyses and visualization of genes and gene ontology (GO). Only those sequences that could be perfectly mapped to sgRNAs of the GeCKO libraries were accounted for in statistical calculations of the differences between samples.

Small hairpin RNA knockdown

Small hairpin RNA (shRNA) sequences were chosen based on their score ranking in the RNA Interference Consortium (TRC) shRNA library (*https://www.broadinstitute.org/rnai-consortium/rnai-consortium-shrna-library*). Several shRNAs targeting the same gene were tested (Supplemental Table S2). For knocking down genes in A375 melanoma and P1F/TERT cells, the shRNAs were expressed by using the lentiviral transfer vector TRC2-pLKO-Puro (MilliporeSigma, Burlington, MA, USA). For knocking down genes in Hermes 4C cells, the shRNAs were expressed by using the lentiviral transfer vector TRC2-pLKO-Hyg or TRC2-pLKO-Bst, which is identical to TRC2-pLKO-Puro except that the puromycin gene was replaced by a hygromycin or blasticidin gene, respectively. Lentivirus particles were packaged as described above. Cells transduced with the viruses were selected with puromycin, hygromycin, and blasticidin at 1, 100, and 10 μg/ml, respectively.

Assay for cisplatin-induced apoptosis

Cells were seeded in 12-well plates (~30% confluence for A375 and ~60% confluence for Hermes 4C and P1F/TERT cells). After 24 h of incubation, the cells were treated with different doses of cisplatin for 24 (A375 cells and derivatives) or 48 h (Hermes 4C and P1F/TERT as well as their derivatives). Attached and floating cells from the same sample were harvested and pooled. After washing with PBS, the cells were stained with Alexa Fluor 488–conjugated annexin V (Thermo Fisher Scientific, Waltham, MA, USA) and analyzed by using flow-cytometry. SE and *P* values

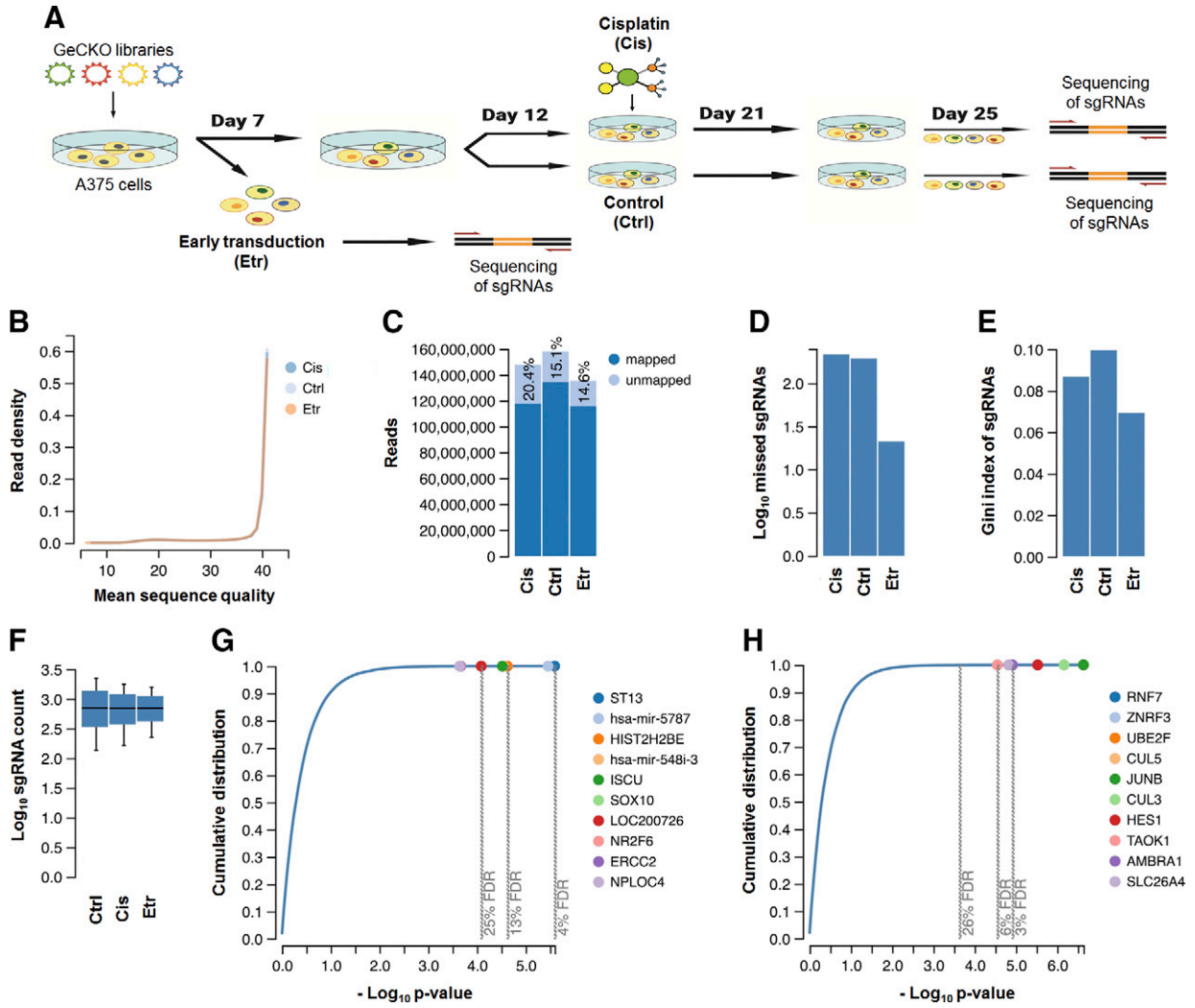

Figure 1. Genome-wide screening of genes implicated in cisplatin resistance or sensitivity in A375 human melanoma cells. *A*) Flow chart of the screening process, showing early transduction cells (Etr), cells treated with cisplatin (Cis), and untreated control cells (Ctrl). *B*) Distribution of sequencing read qualities (Phred score). *C*) sgRNA reads perfectly mapped and unmapped to the GeCKO libraries. *D*) Log_{10} count of missed sgRNAs. *E*) Gini index of sgRNAs, which inversely correlates with sgRNA diversity. *F*) Log_{10} count of sgRNAs. *G*, *H*) Cumulative distribution of the $-\log_{10} P$ values of genes whose disruptions were positively (*G*) or negatively (*H*) selected by cisplatin. The positions of the top 10 disrupted genes positively and negatively selected by cisplatin are indicated in the respective graphs.

(unpaired Student's *t* test) were calculated from data generated from at least 3 independent experiments.

Clonogenic assay

To determine plating efficiencies, 200 A375 melanoma cells with or without specific gene knockdowns were seeded in triplicates in Petri dishes (10 cm in diameter). To determine cisplatin sensitivity, 6000–20,000 cells were seeded in triplicates in the Petri dish. Six hours later (when the cells were attached to the bottom of the container), cisplatin was added to the culture to a final concentration of 1 μM. It appeared that the cells were very sensitive to cisplatin when they were seeded to low densities in the clonogenic assay. After 20 h of treatment, the cells were washed once with complete medium and once with PBS, then replenished with fresh medium. After 9–14 d of incubation, colonies formed were stained with 1% methylene blue (in 50% ethanol) and counted. The survival fractions were calculated by dividing the plating efficiencies of the cisplatin-treated samples by those of the respective untreated samples.

Ariadne-1 homolog and eukaryotic translation initiation factor 4E 2 overexpression

Human ariadne-1 homolog (ARIH1; MHS6278-202802257) and eukaryotic translation initiation factor 4E 2 (EIF4E2; MSH6278-202826512) sequence-verified cDNA plasmids were purchased from Dharmacon (Lafayette, CO, USA). To overexpress ARIH1, the Cas9 gene in the lentiviral vector lentiCRISPR v.2 (10) were replaced with the ARIH1 cDNA. To overexpress EIF4E2, the Cas9 and puromycin genes in lentiCRISPR v.2 were replaced with the EIF4E2 cDNA and the hygromycin gene, respectively. Lentivirus particles expressing the cDNAs were packaged as described above. Cells transduced with the viral particles were selected with 1 μg/ml puromycin or 100 μg/ml hygromycin.

Verteporfin and CA3 treatments

Verteporfin and CA3 were purchased from R&D Systems (Minneapolis, MN, USA) (5305) and Selleckchem (Houston, TX,

USA) (S8661), respectively, and dissolved in DMSO. Cells at ~80% confluence were treated with different concentrations of verteporfin and CA3. After 24–48 h of treatment, the cells were washed with PBS twice, and whole cell proteins extracts were prepared.

Western blot

Approximately 0.8×10^6 cells in a well of a 6-well plate were washed with PBS, scraped off, and pelleted. The cells were then lysed by vortexing in 100 μl of phenol, 5 μl of β-mercaptoethanol, and 100 μl of PBS for 15 min. Proteins in the lysate were precipitated by mixing with 1.2 ml methanol containing 0.1 M ammonium acetate followed by centrifugation at 4°C for 30 min. Proteins were separated on SDS-PAGE gels, transferred onto PVDF membranes, and probed with antibodies against β-actin (sc-47778; Santa Cruz Biotechnology, Dallas, TX, USA), ARIH1 (sc-514551; Santa Cruz Biotechnology), catenin β-1 (CTNNB1; 51067-2-AP; Proteintech, Rosemont, IL, USA), EIF4E2 (sc-100731; Santa Cruz Biotechnology), glyceraldehyde-3-phosphate dehydrogenase (GAPDH; sc-47724; Santa Cruz Biotechnology), histone H4 (04-858; MilliporeSigma), neurofibromin 2 (NF2; A13626; ABclonal, Woburn, MA, USA), p53 (sc-126; Santa Cruz Biotechnology), phosphorylated p53 (9284S; Cell Signaling Technology, Danvers, MA, USA), ring finger protein 7 (RNF7; 11905-1-AP; Proteintech), ubiquitin-conjugating enzyme E2 F (UBE2F; sc-398668; Santa Cruz Biotechnology), yes-associated protein (YAP; sc-376830; Santa Cruz Biotechnology), and zinc and ring finger 3 (ZNRF3) (R2407-1; Abiocode, Agoura Hills, CA, USA).

Quantitative RT-PCR

Total RNA was extracted from the cells using Quick-RNA Miniprep Plus Kit (R1057T; Zymo Research, Irvine, CA, USA). The mRNAs of β-actin (internal control), ARIH1, and EIF4E2 were hybridized to appropriated primers (Supplemental Table S3) and reverse transcribed by using the ProtoScript II First Strand cDNA Synthesis Kit (New England Biolabs, Ipswich, MA, USA). The RNAs in the reverse transcribed samples were digested by using RNase I_f (New England Biolabs), and the cDNAs were purified by using DNA Clean and Concentrator (D4004; Zymo Research). Real-time quantitative PCR of the cDNAs was performed by using the Sybr Select Master Mix (4472908; Thermo Fisher Scientific) and appropriate primers (Supplemental Table S3). The standard curves were generated by using plasmids bearing cDNAs of β-actin (MHS6278-202755711), EIF4E2 (MHS6278-202826512), and ARIH1 (MHS6278-202802257) (Dharmacon).

RESULTS

Genome-wide CRISPR-Cas9 knockout screening of genes and biologic processes implicated in cisplatin resistance

To identify novel genes implicated in cisplatin resistance, we performed genome-wide gene disruption screening in A375 human melanoma cells by using the human GeCKO v.2 lentiviral pooled libraries, which encode $\sim 1.2 \times 10^5$ unique sgRNAs targeting 99.4% of all human genes (6 sgRNAs per gene and up to 4 sgRNAs per miRNA) (10). After the sgRNA-targeted gene disruption events had occurred, a fraction of the cells were treated with cisplatin to kill ~50–60% of the cells (Fig. 1*A*). The cisplatin-treated and untreated cells were passaged synchronously to ensure they underwent similar numbers of cell divisions before harvesting. Total genomic DNA was isolated from the early transduction and cisplatin-treated and untreated control cells. The sgRNA-encoding sequences integrated into the genome were sequenced and analyzed by using MAGeCK-VISPR, a comprehensive quality control, analysis, and visualization workflow for CRISPR screens (9, 11). Most of our sequencing reads are of high quality (Fig. 1*B*). Over 110 million reads from each of the treatment groups were perfectly mapped to the sgRNAs contained in the GeCKO libraries (Fig. 1*C*) with excellent distribution and coverage (Fig. 1*D–F*). Indeed, only 21 out of the 1.2×10^5 sgRNAs were missing in the early transduction cells. Only those sgRNAs that could be perfectly mapped to the GeCKO libraries were accounted for in statistical calculations of the differences between samples. The disrupted genes positively and negatively selected by cisplatin were assessed by testing whether their targeting sgRNA abundance differed significantly between the cisplatin-treated and untreated control samples. The cumulative distributions of $-\log_{10} P$ values of the genes whose disruptions were positively (*i.e.*, with their targeting sgRNAs enriched) and negatively (*i.e.*, with their targeting sgRNAs diminished) selected by cisplatin treatment are shown in Fig. 1*G*, *H*, respectively. The top disrupted genes positively and negatively selected by cisplatin are listed in Supplemental Tables S4 and S5, respectively.

The disrupted genes causing decreased (lethality or slow growth) or on rare occasions increased cell fitness (fast growth) were assessed by testing whether their targeting sgRNA abundance differed significantly between the early transduction and untreated control samples (**Fig. 2** and Supplemental Table S6). A substantial fraction of the disrupted genes positively or negative selected by cisplatin overlap with those causing decreased or increased fitness, respectively. However, no overlap exists between disrupted genes positive selected by cisplatin and those causing increased fitness, or between those negatively selected by cisplatin and those causing decreased fitness (Fig. 2). These results indicate that fast and slow cell growth may cause cisplatin sensitivity and resistance, respectively.

To assess the biologic processes implicated in cisplatin resistance, we performed GO enrichment analyses by using VISPR, which activates Gene Ontology Enrichment Analysis and visualization (GORILLA) and takes the whole ranked list of genes based on the *P* values reported by the "count" and "test" functions of MAGeCK to perform a threshold-free enrichment analysis (11). Protein translation, mitochondrial respiratory chain complex assembly, signal recognition particle–dependent cotranslational protein targeting to membrane, and mRNA catabolic processes were the top disrupted biologic processes positively selected by cisplatin (Supplemental Fig. S1 and Supplemental Table S7), indicating that these processes are responsible for cisplatin sensitivity and that disruption of them leads to cisplatin resistance. In contrast, proteasome-mediated ubiquitin-dependent protein catabolic process, negative regulations of cellular catabolic

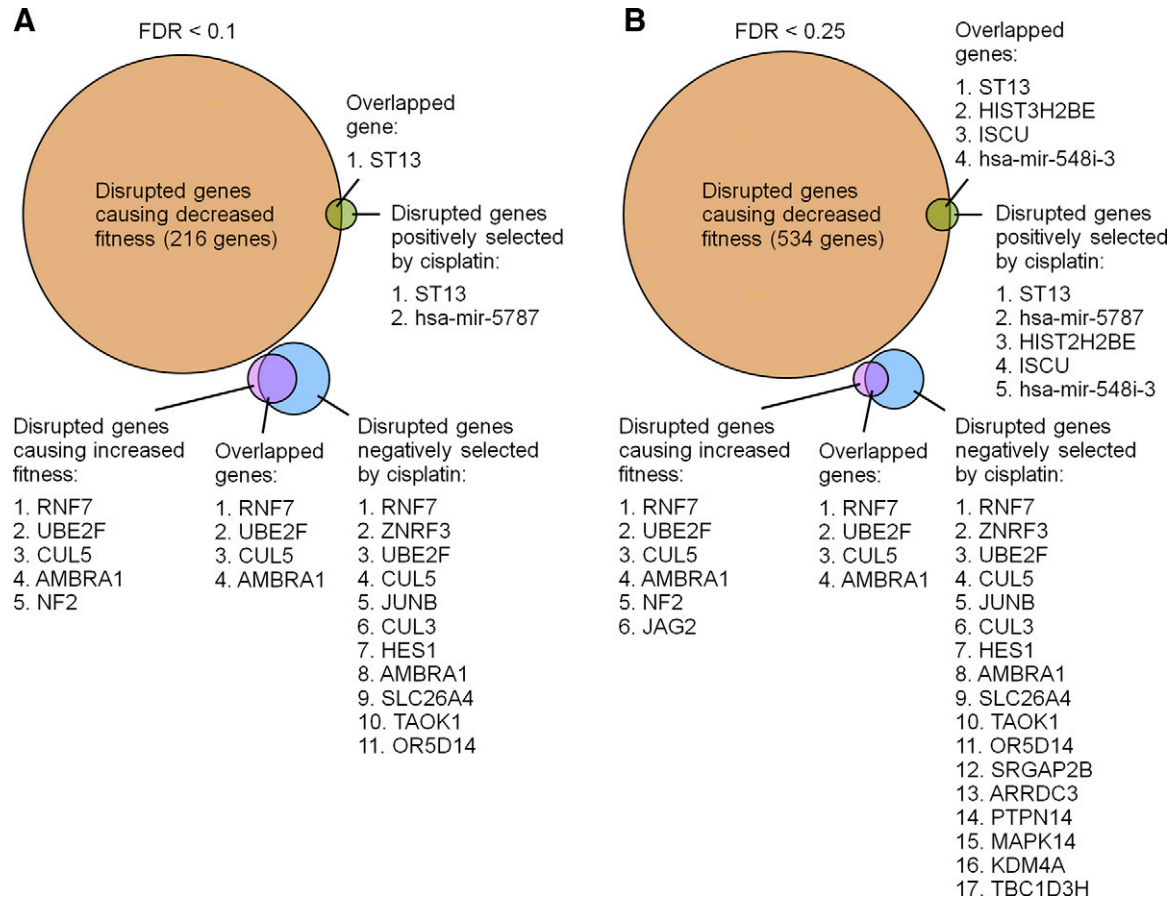

Figure 2. Disrupted genes positively and negative selected by cisplatin overlap with those causing decreased and increased cell growth (fitness), respectively, for A375 cells. *A*) Disrupted genes with an FDR <0.1. *B*) Disrupted genes with an FDR <0.25.

process, and regulation of cellular protein localization were the top disrupted biologic processes negatively selected by cisplatin (Supplemental Fig. S2 and Supplemental Table S8), indicating that these processes are responsible for cisplatin resistance and that disruption of them leads to cisplatin sensitivity.

Neither DNA repair pathways nor drug transport systems were found to be among the top biologic processes selected by cisplatin (Supplemental Tables S7 and S8). The VISPR-activated GORILLA analysis allows a maximum enrichment *P* value of 0.001, which would miss the biologic processes with a higher *P* value. To assess if DNA repair contributes to cisplatin resistance to a certain extent, we performed MAGeCK pathway enrichment analyses against the current 4437 gene sets of GO biologic processes. The MAGeCK pathway enrichment analyses also take the whole ranked list of genes based on the *P* values reported by the "test" function of MAGeCK. Among the different DNA repair pathways, nucleotide excision repair and postreplication repair appeared to contribute the most to cisplatin resistance (Supplemental Table S9). This is not unexpected, because nucleotide excision repair factors are well known to be involved in removal of cisplatin-induced intra- and interstrand crosslinks, and postreplication repair is responsible for tolerance to DNA damage (12). Other DNA repair pathways appeared to contribute little to cisplatin resistance (Supplemental Table S9).

Knockdown of the top negatively selected genes also sensitizes A375 melanoma and melanocyte cells to cisplatin

Our genome-wide knockout screening indicates that RNF7, ZNRF3, and UBE2F are the top 3 disrupted genes negatively selected by cisplatin (Supplemental Table S5). ZNRF3 is an E3 ubiquitin ligase that is known to negatively regulate the Wnt signaling pathway (13). UBE2F is an E2 neural precursor cell expressed, developmentally down-regulated 8–conjugase involved in neddylation of cullin 5, the core component of multiple Skp, cullin, F-box–containing complex–like Elongin-Cullin-SOCS E3 ubiquitin-protein ligase complexes (14). RNF7 is a probable component of the Skp, cullin, F-box–containing complex E3 ubiquitin ligase complex that also promotes neddylation of cullin 5 *via* its interaction with UBE2F (14). To determine if our screening results were valid, we knocked down the top 3 negatively selected genes in A375 cells by using lentivirus-based shRNAs (**Fig. 3*A*–*C***). Indeed, knockdown any of these genes caused significant increase of cell apoptosis (Fig. 3*D*, *E*) and decrease of cell survival (Fig. 3*F*) upon cisplatin treatment.

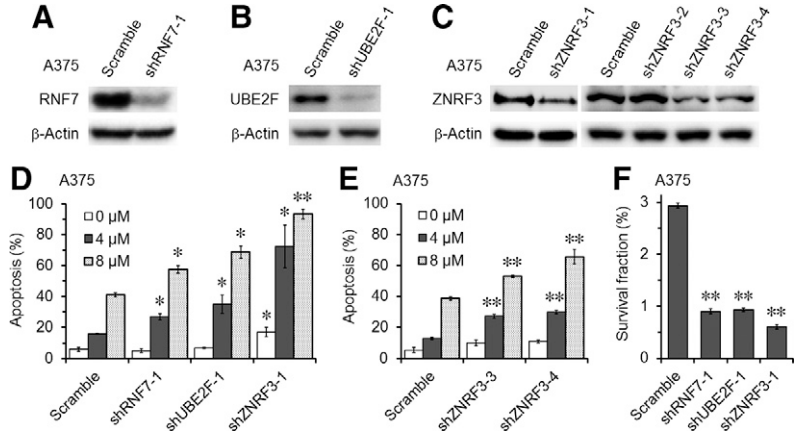

Figure 3. Confirmation of the top 3 disrupted genes negatively selected by cisplatin in A375 melanoma cells. *A–C*) Western blot showing knockdown of the genes by shRNAs, including RNF7-targeting shRNA (shRNF7) (*A*), UBE2F-targeting shRNA (shUBE2F) (*B*), and ZNRF3-targeting shRNA (shZNRF3) (*C*). β-Actin serves as loading control. *D*, *E*) Cisplatin-induced apoptosis in cells expressing the indicated shRNAs. *F*) Clonogenic assay showing survival fraction (%) of A375 melanoma cells expressing the indicated shRNAs after treatment with 1 μM of cisplatin. Note that the cells were very sensitive to cisplatin when they were seeded to low densities in the clonogenic assay. Error bars stand for SE. $*P < 0.05$; $**P < 0.001$; Student's *t* test, between samples of the indicated knockdown and scramble shRNAs at the respective cisplatin doses.

To determine if the implications of ZNRF3, RNF7, and UBE2F in cisplatin resistance are limited to the melanoma cells, we knocked down these genes in the Hermes 4C human immortalized melanocytes (5, 6) (**Fig. 4*A–C***). ZNRF3 or UBE2F knockdown significantly sensitized the melanocytes to cisplatin. However, RNF7 knockdown slightly (statistically insignificant) sensitized the melanocytes to cisplatin (Fig. 4*D*).

Sensitization of melanoma and melanocyte cells to cisplatin by ZNRF3 depletion is not due to CTNNB1 up-regulation but can be suppressed by CTNNB1 depletion

ZNRF3 and its highly homologous ubiquitin ligase ring finger protein 43 (RNF43) are known to be the targets and negative feedback regulators of the Wnt signaling pathway by mediating ubiquitination and subsequent degradation of Frizzled and LDL receptor–related proteins 5 and 6 (LRP5/6), the receptor and coreceptor for Wnt (**Fig. 5*A***) (15). The Wnt signaling is categorized into β-catenin–dependent (canonical) and independent (noncanonical) pathways (16). The canonical Wnt signaling pathway is activated upon binding of Wnt ligands to the Frizzled and LRP5/6, which causes translocation of the β-catenin destruction complex to the plasma membrane, thereby preventing phosphorylation and degradation of β-catenin (Fig. 5*A*). Accumulation and translocation of β-catenin into the nucleus stimulates transcription of over 100 genes, including ZNRF3 and RNF43 (15). Fundamentally, activated Wnt–β-catenin signaling enhances cell proliferation by promoting cell cycle progression (17).

To determine if ZNRF3 modulates cisplatin resistance by regulating Wnt–β-catenin signaling, we knocked down ZNRF3 and CTNNB1 (the β-catenin gene) individually or simultaneously (Fig. 5*B*, *C*). None of the shZNRF3s, including shZNRF3-1, shZNRF3-3, and shZNRF3-4, that could significantly knock down ZNRF3 (Fig. 3C) caused significant up-regulation of CTNNB1 in the A375 and Hermes 4C cells (Fig. 5*B*, *C*). We also found that disruption or depletion of ZNRF3 did not affect cell growth, indicating that the Wnt–β-catenin signaling was not significantly activated upon ZNRF3 disruption or depletion. Our results are in line with the previous report showing that only codepletion of ZNRF3 and RNF43 causes significant up-regulation of CTNNB1 (18). Presumably, the CTNNB1 level was maintained through the negative feedback mechanism in which the knockdown of ZNRF3 was compensated for by up-regulation of RNF43. Interestingly, the A375 melanoma and Hermes 4C melanocyte cells with ZNRF3 and CTNNB1 double knockdowns were more cisplatin resistant than those with ZNRF3 single knockdown (Fig. 5*D*, *E*). As expected, the levels of total and phosphorylated p53, the key factor involved in cell apoptosis, were increased upon cisplatin treatment (Fig. 5*F*, *G*). ZNRF3 knockdown caused more dramatic increase of total and phosphorylated p53 upon cisplatin treatment (Fig. 5*F*, *G*). However, the p53 level was reduced in cells with

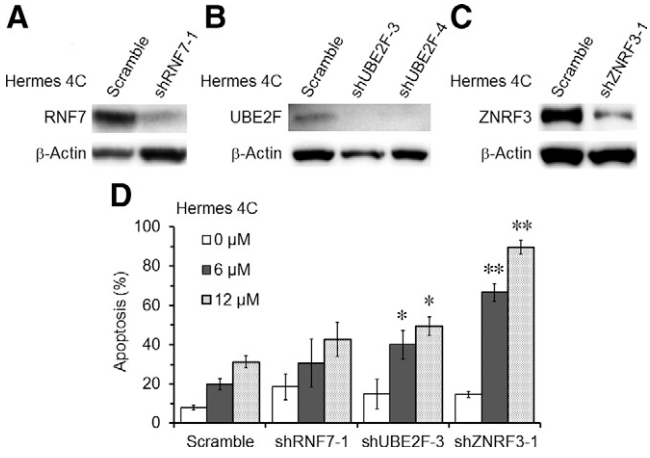

Figure 4. Knockdown of ZNRF3, RNF7, or UBE2F in Hermes 4C melanocytes also cause different degrees of cisplatin sensitivity. *A–C*) Western blot showing knockdown of the genes by shRNAs, including RNF7-targeting shRNA (shRNF7) (*A*), UBE2F-targeting shRNA (shUBE2F) (*B*), and shZNRF3 (*C*). β-Actin serves as loading control. *D*) Cisplatin-induced apoptosis. Error bars stand for SE. $*P < 0.05$; $**P < 0.001$; Student's *t* test, between samples of the indicated knockdown and scramble shRNAs at the respective cisplatin doses.

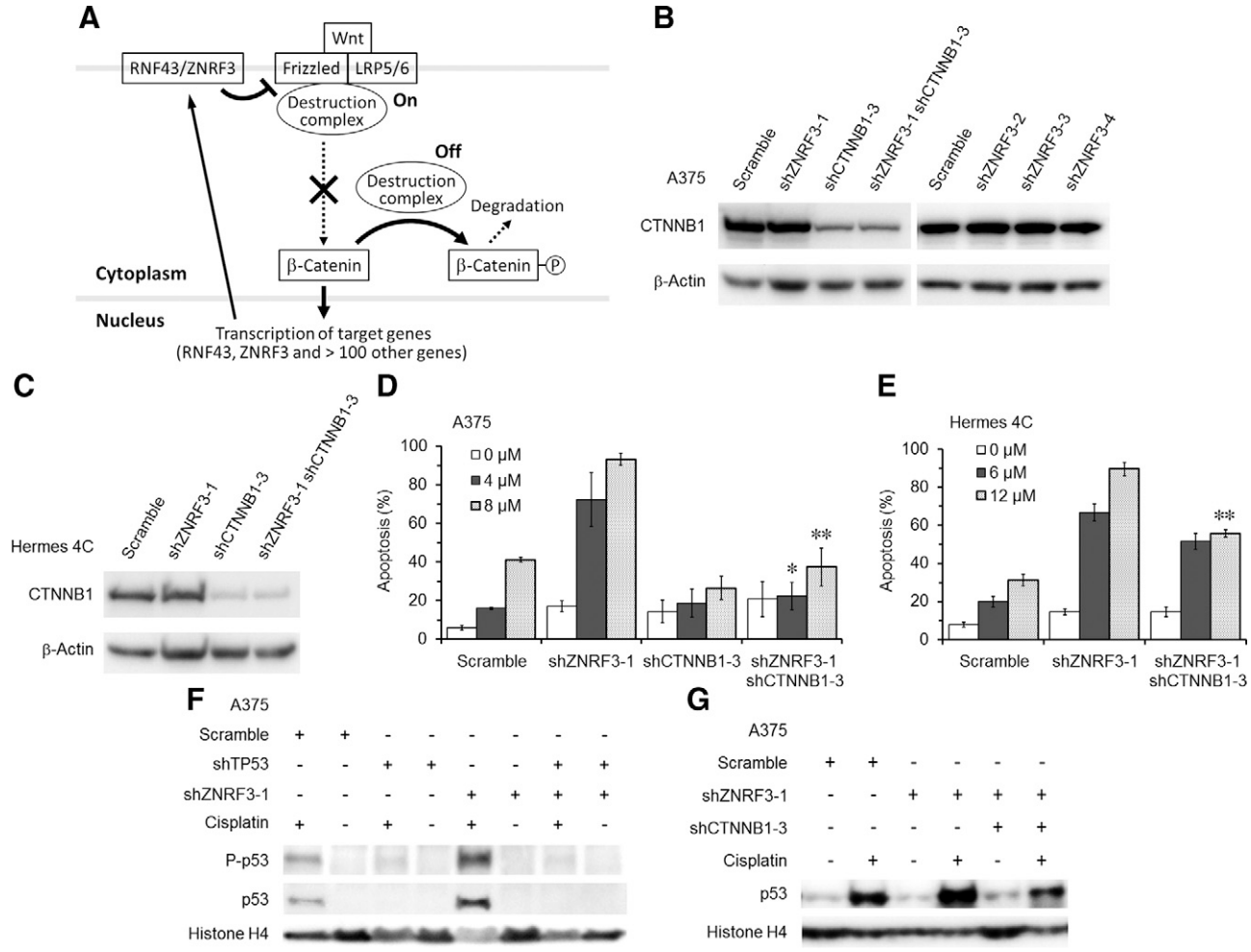

Figure 5. Sensitization of cells to cisplatin by ZNRF3 knockdown is not due to CTNNB1 up-regulation but can be suppressed by CTNNB1 depletion. *A*) Simplified schematic of Wnt–β-catenin signaling. *B*, *C*) Western blots showing CTNNB1 (β-catenin) protein in A375 (*B*) and Hermes 4C (*C*) cells with individual and double knockdowns of ZNRF3 and CTNNB1. *D*, *E*) Cisplatin-induced apoptosis of A375 (*D*) and Hermes 4C (*E*) cells with the indicated shRNA knockdowns. Error bars stand for SE. $*P < 0.05$; $**P < 0.001$; Student's *t* test, between samples of the ZNRF3 and CTNNB1 double knockdown and ZNRF3 single knockdown at the respective cisplatin doses. *F*, *G*) Western blots showing total and phosphorylated p53 (P-p53) in A375 cells with the indicated shRNA knockdowns before and after cisplatin treatment. β-Actin or histone H4 serves as loading control. shCTNNB1, CTNNB1-targeting shRNA.

ZNRF3 and CTNNB1 double knockdown compared with that in cells with ZNRF3 single knockdown (Fig. 5*F*, *G*).

Taken together, our results indicate that the sensitization of melanoma and melanocyte cells to cisplatin by ZNRF3 depletion is not due to up-regulation of CTNNB1. However, the sensitization can still be suppressed by CTNNB1 depletion, which enhances cisplatin resistance.

Knockdown of NF2 sensitizes A375 melanoma but not normal cells to cisplatin

We noticed that NF2 (also known as merlin) was ranked 22 among the disrupted genes negatively selected by cisplatin in A375 melanoma cells (Supplemental Table S5). However, 3 (A_31760, A_31761, and B_31719) out of 6 NF2-targeting sgRNAs were highly negatively selected, whereas the other 3 sgRNAs were not significantly present in the control and cisplatin-treated cells (**Fig. 6*A***). The assessment of positively or negatively selected genes is affected by the presence and cutting efficiency of different sgRNAs present in the GeCKO libraries. If some of the 6 sgRNAs targeting a gene were absent, present at a low level, or with low cutting efficiency, then a high *P* value, false discovery rate (FDR), or both would be assigned to the gene. We therefore tested if disruption of NF2 was truly negatively selected by cisplatin. Indeed, NF2 knockdown sensitized A375 melanoma cells to cisplatin (Fig. 6*B*, *E*, *H*).

To determine if the implication of NF2 in cisplatin resistance is limited to the melanoma cells, we knocked down this gene in the Hermes 4C melanocytes (Fig. 6*C*) and P1F/TERT (Fig. 6*D*) cells. In contrast to the A375 melanoma cells (Fig. 6*E*), the Hermes 4C cells (Fig. 6*F*) became slightly (statistically insignificant) more resistant to cisplatin, whereas the P1F/TERT cells (Fig. 6*G*) became significantly more resistant to cisplatin. The levels of total or phosphorylated p53 were not

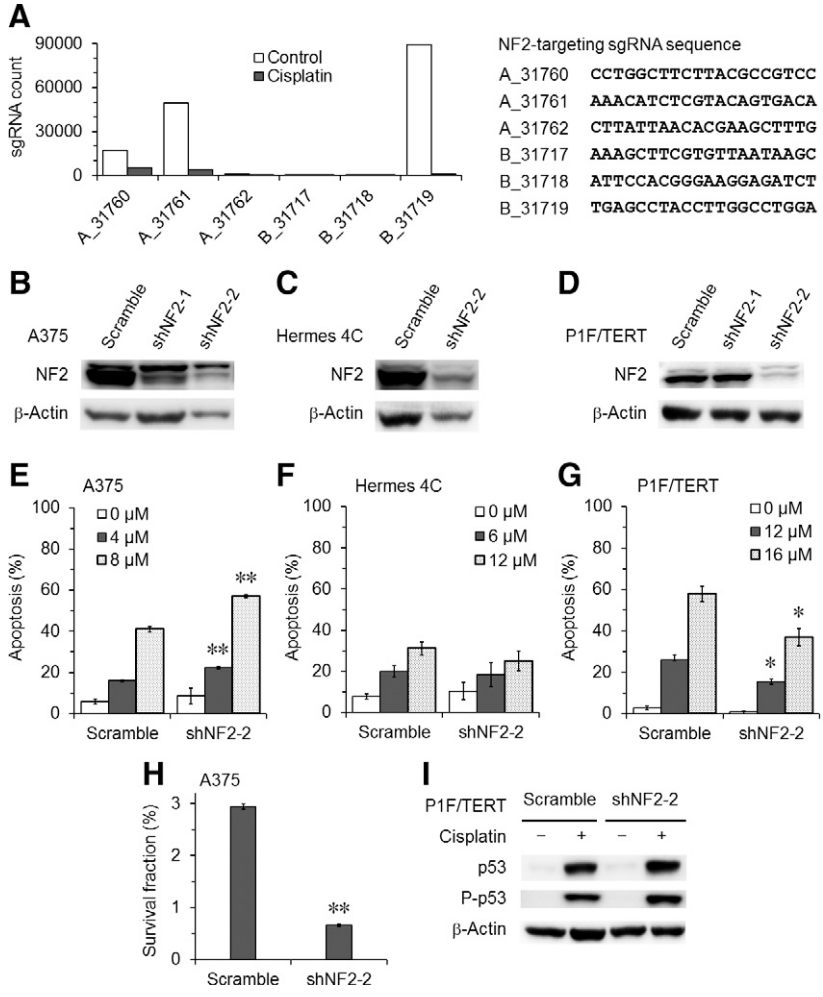

Figure 6. NF2 knockdown sensitizes the A375 melanoma cells but not Hermes 4C melanocyte and P1F/TERT fibroblast cells to cisplatin. *A*) Counts of the 6 NF2-targeting sgRNAs in the control and cisplatin-treated A375 cells. The sequences of the 6 sgRNAs are shown on the right. *B–D*) Western blots showing NF2 knockdown in the A375 (*B*), Hermes 4C (*C*), and P1F/TERT (*D*) cells. *E–G*) Cisplatin-induced apoptosis of A375 (*E*), Hermes 4C (*F*), and P1F/TERT (*G*) cells with NF2 knockdown. Error bars stand for SE. $*P < 0.05$; $**P < 0.001$ (Student's *t* test), between samples of the indicated knockdown and scramble shRNAs at the respective cisplatin doses. *H*) Clonogenic assay showing survival fraction (%) of A375 melanoma cells after treatment with 1 μM of cisplatin. Note that the cells were very sensitive to cisplatin when they were seeded to low densities in the clonogenic assay. Error bars stand for SE. $**P < 0.001$ (Student's *t* test), between the samples of shNF2-2 and scramble shRNA. *I*) Western blots showing total and phosphorylated p53 (P-p53) in P1F/TERT cells with the indicated shRNA knockdowns before and after cisplatin treatment. β-Actin serves as loading control. shNF2, NF2-targeting shRNA.

significantly affected by NF2 knockdown (Fig. 6*I*), indicating that the modulation of cisplatin sensitivity by NF2 is independent of p53.

NF2 and YAP regulate the levels of ARIH1 and EIF4E2

NF2 regulates multiple signaling pathways, including the Hippo pathway (**Fig. 7*A***) (19, 20). YAP is a potent transcription coactivator and the main downstream target of the Hippo pathway, acting *via* binding to the transcriptional enhancer associated domain (TEAD) transcription factor. YAP can be phosphorylated by large tumor suppressor kinases 1 and 2 and then degraded in the cytoplasm. In certain cell types, NF2 may down-regulate YAP by promoting its phosphorylation and degradation. We searched for NF2-regulated factors that might be implicated in cisplatin resistance. We found that EIF4E2 (also called 4EHP), which represses global translation initiation by competing with eukaryotic translation initiation factor 4E for binding to the mRNA cap (21), and ARIH1, an E3 ubiquitin ligase that promotes binding of EIF4E2 to the mRNA cap by ubiquitinating EIF4E2 in response to DNA damage (22), were barely detectable in the Hermes 4C melanocyte and P1F/TERT fibroblast cells but were highly expressed in A375 melanoma cells (Fig. 7*B*). Upon NF2 knockdown, both EIF4E2 and ARIH1 were up-regulated in Hermes 4C and P1F/TERT cells (Fig. 7*B*). The up-regulations were not due to increased transcription because the mRNA levels of ARIH1 and EIF4E2 were not significantly changed upon NF2 knockdown (Fig. 7*C*). In contrast to the normal cells, the A375 melanoma cells showed decreased ARIH1 and unchanged EIF4E2 upon NF2 knockdown (Fig. 7*B*).

The levels of YAP correlated well with those of ARIH1 and EIF4E2, being high in A375 cells and low in Hermes 4C and P1F/TERT cells (Fig. 7; compare *B* and *D*). However, in contrast to those of ARIH1 and EIF4E2 (Fig. 7*B*), the level of YAP was not significantly affected by NF2 knockdown (Fig. 7*D*), indicating NF2 does not regulate YAP in these cells. To examine if ARIH1 and EIF4E2 expressions are affected by YAP, we treated the cells with verteporfin, a highly specific inhibitor of YAP-TEAD interaction (Fig. 7*A*) (23). The levels of ARIH1 and EIF4E2 were greatly reduced in P1F/TERT (with NF2 knockdown) (Fig. 7*E*, *F*) and A375 cells (Fig. 7*G*, *H*) upon verteporfin treatment. Treatment of the cells with CA3, a more potent and specific inhibitor of YAP1 (24), also caused reduction of ARIH1 and EIF4E2 (Fig. 7*I–L*). These results indicate that YAP up-regulates ARIH1 and EIF4E2 in both the normal and melanoma cells.

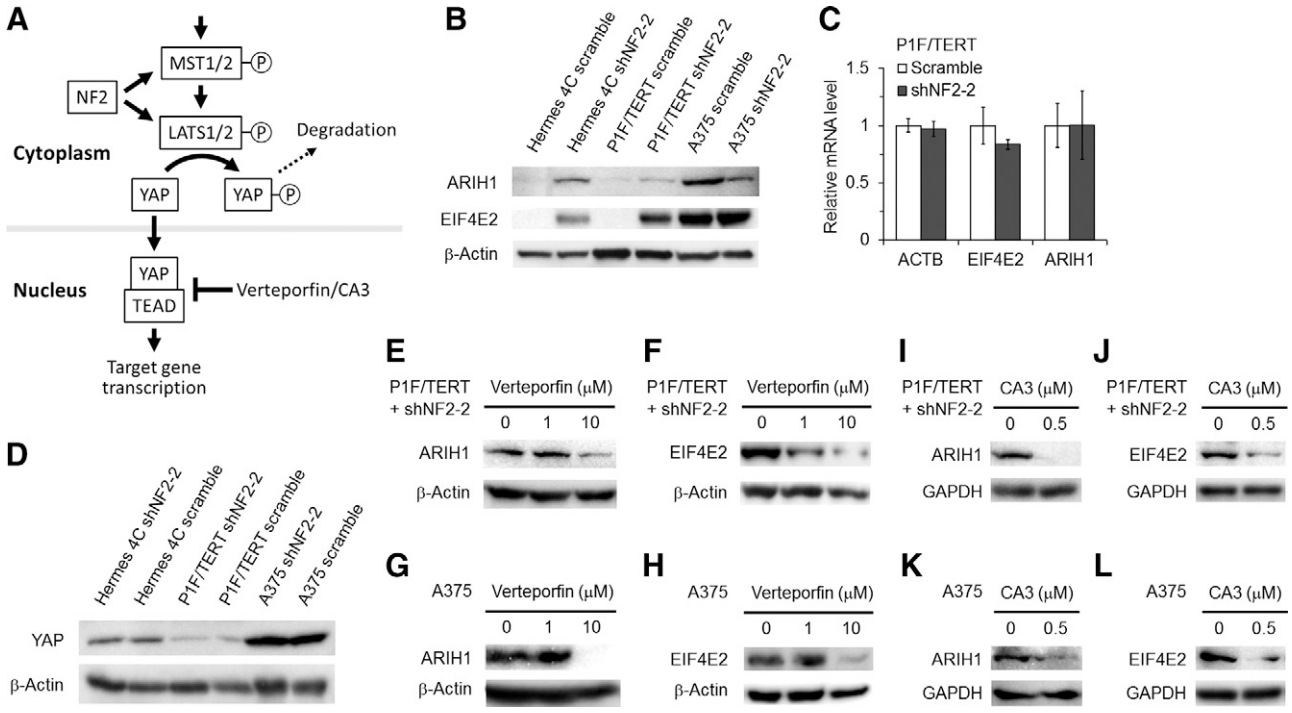

Figure 7. Regulation of ARIH1 and EIF4E2 by NF2 and YAP. *A*) Simplified schematic of Hippo signaling. LATS1/2, large tumor suppressor kinases 1 and 2; MST1/2, mammalian sterile 20–like kinases 1 and 2. *B*) Western blots showing levels of ARIH1 and EIF4E2 in the indicated cells with or without NF2 knockdown. *C*) Relative levels of the indicated mRNAs in P1F/TERT cells with or without NF2 knockdown. The data were obtained by reverse transcription quantitative PCR. Error bars stand for SE. *D*) Western blot showing YAP levels in the indicated cells with or without NF2 knockdown. *E–H*) Western blots showing ARIH1 and EIF4E2 in the indicated cells following treatment with verteporfin, the inhibitor of YAP-TEAD interaction. *I–L*) Western blots showing ARIH1 and EIF4E2 in the indicated cells following treatment with CA3, a potent and specific YAP1 inhibitor. β-Actin (ACTB) or GAPDH serves as loading control. shNF2, NF2-targeting shRNA.

Taken together, our results indicate that the levels of ARIH1 and EIF4E2 are regulated by both NF2 and YAP. However, the regulation of ARIH1 and EIF4E2 by NF2 is not *via* regulating YAP. Although YAP up-regulates ARIH1 and EIF4E2 in all the cells, NF2 regulates these factors differently between the normal and melanoma cells.

ARIH1 but not EIF4E2 is implicated in cisplatin resistance

To determine if up-regulation of ARIH1 or EIF4E2 increase cisplatin resistance, we overexpressed these factors in P1F/TERT cells, which normally express very low levels of these factors (Figs. 7*B* and **8*A***). Neither EIF4E2 nor ARIH1 overexpression affected NF2 expression (Fig. 8*A*), indicating that the regulation of EIF4E2 and ARIH1 by NF2 is unidirectional (*i.e.*, no feedback regulation). Overexpression of ARIH1 but not EIF4E2 dramatically increased cellular resistance to cisplatin (Fig. 8*B*). Similar to NF2 knockdown, ARIH1 or EIF4E2 overexpression did not dramatically affect the levels of total p53 or the phosphorylated p53 (compare Figs. 6*I* and 8*C*). Collectively, these results indicate that the modulation of cisplatin sensitivity by NF2 may be *via* regulating ARIH1 and is largely independent of p53.

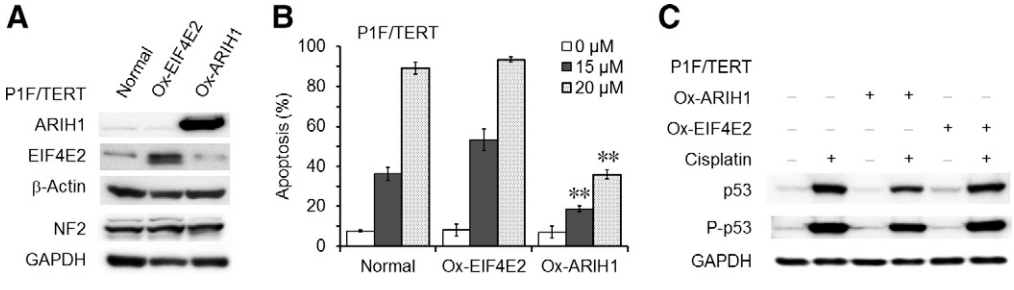

Figure 8. Overexpression of ARIH1 but not EIF4E2 causes cisplatin resistance. *A*) Western blots showing ARIH1, EIF4E2, and NF2 in P1F/TERT cells normally expressing or overexpressing ARIH1 (Ox-ARIH1) or EIF4E2 (Ox-EIF4E2). *B*) Cisplatin-induced apoptosis of P1F/TERT cells normally expressing or overexpressing ARIH1 or EIF4E2. Error bars stand for SE. $^{**}P < 0.001$ (Student's *t* test), between samples of the indicated overexpressions and normal expression at the respective cisplatin doses. *C*) Western blots showing total and phosphorylated p53 (P-p53) in P1F/TERT cells with the indicated gene overexpressions before and after cisplatin treatment. GAPDH serves as loading control.

DISCUSSION

Biologic processes responsible for cisplatin sensitivity and resistance

We screened for genes and biologic processes positively and negatively selected by cisplatin when they are disrupted. Among the top positively selected biologic processes are protein translation, mitochondrial respiratory chain complex assembly, signal recognition particle–dependent cotranslational protein targeting to membrane, and mRNA catabolic processes, indicating that these processes are normally responsible for cisplatin sensitivity. To the best of our knowledge, these biologic processes have not been generally recognized as the leading contributors of cisplatin sensitivity. Protein synthesis consumes a lion's share of energy and cellular resources. When cells are under stress, protein translation is globally repressed except for certain stress proteins (25, 26). The so-called translational reprogramming may lie at the heart of the stress response and is required for rapid cellular adaptation under stress (26). Therefore, disruption of genes that are not essential for cell viability but are involved in protein translation may allow the cell to better adapt to cisplatin-induced cellular stress. Also, slow cycling can be a common feature of melanoma cells that are drug resistant (27). Disruptions of protein translation, cotranslational targeting to destination membrane, and mitochondrial respiratory chain complex assembly may generally slow down cell cycling, leading to cisplatin resistance. Indeed, we found that a substantial fraction of the top disrupted genes that are positively selected by cisplatin largely overlap with those causing decreased fitness (Fig. 2). Also, mitochondrial dysfunction has been shown to enhance cisplatin resistance (28, 29). Disruption of mitochondrial respiratory chain complex assembly may impair mitochondrial function, leading to enhanced cisplatin resistance. Furthermore, global mRNA decay has been found in recent years to occur early in apoptosis, preceding membrane lipid scrambling, genomic DNA fragmentation, and apoptotic changes to translation initiation factors (30). Therefore, disruption of the mRNA catabolic process may impair the apoptosis process, leading to cisplatin resistance.

We found that the top disrupted biologic processes negatively selected by cisplatin are proteasome-mediated ubiquitin-dependent protein catabolic process, negative regulations of cellular catabolic process and regulation of cellular protein localization, indicating that these processes are normally responsible for cisplatin resistance. Our findings are in line with the notion that inhibitors of apoptosis proteins are E3 ubiquitin ligases regulating caspase activity that is required for apoptosis (31–33). Also, in contrast to disruption of protein translation and cotranslational targeting to membrane, disruption of the ubiquitin-dependent protein catabolic process and impairment of the negative regulations of cellular catabolic process may impair cellular adaptation to stress and enhance cell proliferation, leading to increased sensitivity to cisplatin.

Alteration of DNA repair pathways have been well known to be implicated in cisplatin resistance (1, 3). However, none of these DNA repair pathways is near the top of biologic processes negatively selected by cisplatin, although disruption of nucleotide excision repair and postreplication repair might mildly sensitize the cells to cisplatin (Supplemental Table S9). One explanation is that only ~1% of intracellular cisplatin forms covalent bonds with nuclear DNA, and the majority of the drug molecules exert their cytotoxicity in the cytoplasm (1). In addition to targeting DNA, cisplatin also causes damage to RNAs, proteins, phospholipids, and carbohydrates (34). Therefore, compared with other biologic processes, the DNA repair pathways may only contribute a small fraction to the cisplatin resistance. It should also be noted that our screening might have missed certain genes. The CRISPR-Cas9 screening relies on disruption of genes, which will miss the genes that are essential for cell viability. Some genes may not be identified if some or all of its targeting sgRNAs are absent or present at low levels in the GeCKO libraries, or with low cutting efficiency. Furthermore, the CRISPR-Ca9 may have off-targets, which may mask or offset the effects of certain genes on cisplatin resistance or sensitivity.

Implications of ZNRF3, CTNNB1, and p53 in cisplatin resistance

We found that the sensitization of cells to cisplatin by ZNRF3 depletion is not due to CTNNB1 up-regulation. Still, the sensitization can be suppressed by depletion of CTNNB1. In view of our finding that slow cell growth may increase cisplatin resistance and the fact that Wnt–β-catenin signaling fundamentally promotes cell growth (17), the suppression of cisplatin sensitivity by depletion of CTNNB1 might be simply due to decreased cell growth. Besides targeting Frizzled and LRP5/6 for degradation, ZNRF3 may have an as-yet unidentified target that is implicated in cisplatin sensitivity. Because ZNRF3 disruption or depletion does not significantly affect cell growth, the unidentified ZNRF3 target is unlikely a factor downstream of CTNNB1 in the Wnt–β-catenin signaling cascade.

p53 is best known for its ability to promote cell cycle arrest and apoptosis (35). We found that ZNRF3 knockdown caused more dramatic increase of total and phosphorylated p53 upon cisplatin treatment. However, the p53 level was reduced in cells with ZNRF3 and CTNNB1 double knockdown compared with that in cells with ZNRF3 single knockdown. These results support the notion that the sensitization of the cells to cisplatin by ZNRF3 knockdown might be in part due to increased activation of p53. However, the roles of p53 are multifaceted, and under certain circumstances p53 may inhibit apoptosis. Indeed, it has been shown that depletion of intracellular NO, which inhibits cisplatin-induced p53 accumulation, or expression of a dominant-negative p53, enhances cisplatin-induced apoptosis in A375 cells (36). Therefore, the underlying mechanism of ZNRF3 in regulating cisplatin sensitivity may be complex, and the contribution of p53 activation to the process remains to be understood.

Implications of NF2, YAP, and ARIH1 in cisplatin resistance

NF2 is implicated in many signaling pathways, including Hippo, epidermal growth factor receptor, Ras, Rac, mechanistic target of rapamycin, focal adhesion kinase–steroid receptor coactivator, PI3K, and lin-28 homolog B (19, 20). Mutations of NF2 are associated with nervous system tumors as well as several other malignant cancers, including melanomas. To the best of our knowledge, if and how NF2 modulates cisplatin sensitivity has not been documented. NF2 is required for proliferation arrest and apoptosis in developing imaginal discs (37). Loss of NF2 has been shown to protect cardiac myocytes from apoptosis stimulated by β adrenergic receptor (38) and pancreatic β cells from apoptosis associated with diabetes (39). Therefore, NF2 appears to be a proapoptotic factor in normal (noncancer) cells, in line with its role as a tumor suppressor. However, we found that NF2 disruption sensitized A375 melanoma cells but not normal cells to cisplatin (Fig. 6), indicating that NF2 becomes an antiapoptotic factor in cancer cells. Whether the antiapoptotic function of NF2 is common to cancers or limited to a subset of cancers remains to be determined. A better understanding of this issue may be very important for development of treatments that specifically kill cancer cells while minimizing toxicity to normal cells.

Up-regulation of YAP, the downstream effector of the Hippo signaling, has been known to cause resistance of multiple types of cancer cells to cisplatin (40–43). Also, down-regulation of mammalian sterile 20–like kinases 1 and 2, the core components of the Hippo pathway that inhibits YAP, has been shown to cause resistance of prostate cancer cells to cisplatin (44). Interestingly, we found that the YAP level is not significantly regulated by NF2 in the melanocyte, fibroblast, and melanoma cells we tested. The regulation of the Hippo signaling can be tissue specific (19). It is possible that NF2 does not significantly regulate the Hippo signaling in the cell types we tested.

ARIH1 has been shown recently to be widely overexpressed in cancer cells, notably in breast and lung adenocarcinomas, and to protect against cisplatin-induced cell death by promoting clearance of damaged mitochondria (mitophagy) (45). ARIH1 has also been shown to protect against cisplatin-induced apoptosis by ubiquitinating EIF4E2, irrespective of the status of p53 or caspase-3 (22). The ubiquitinated EIF4E2 promotes translation arrest by competing with eukaryotic translation initiation factor 4E for binding to the mRNA cap (22). In agreement with the previous reports, we found that ARIH1 is overexpressed in A375 melanoma cells and contributes to cisplatin resistance in a p53-independent manner. This agrees well with the notion that down-regulation of global protein translation enhances cisplatin resistance. Interestingly, we also found that ARIH1 is regulated by both NF2 and YAP, and the roles of NF2 and YAP in modulating cisplatin resistance are at least partially achieved by regulating ARIH1. Furthermore, we found that the regulation of ARIH1 by NF2 is not at the transcription step and is not *via* YAP. The molecular mechanisms by which NF2 and YAP regulate ARIH1 remain to be elucidated. Insights into these mechanisms may also be informative for development of novel cancer treatment strategies. FJ

ACKNOWLEDGMENTS

The authors thank Rutao Cui (Boston University, Boston, MA, USA) for critical comments on the manuscript. This study was supported by the U.S. National Science Foundation (MCB-1615550). The authors declare no conflicts of interest.

AUTHOR CONTRIBUTIONS

T. Ko and S. Li designed the research; T. Ko performed the research; and T. Ko and S. Li analyzed the data and wrote the manuscript.

REFERENCES

1. Galluzzi, L., Vitale, I., Michels, J., Brenner, C., Szabadkai, G., Harel-Bellan, A., Castedo, M., and Kroemer, G. (2014) Systems biology of cisplatin resistance: past, present and future. *Cell Death Dis.* **5**, e1257
2. Winter, C., and Albers, P. (2011) Testicular germ cell tumors: pathogenesis, diagnosis and treatment. *Nat. Rev. Endocrinol.* **7**, 43–53
3. Ferreira, J. A., Peixoto, A., Neves, M., Gaiteiro, C., Reis, C. A., Assaraf, Y. G., and Santos, L. L. (2016) Mechanisms of cisplatin resistance and targeting of cancer stem cells: adding glycosylation to the equation. *Drug Resist. Updat.* **24**, 34–54
4. Mattia, G., Puglisi, R., Ascione, B., Malorni, W., Carè, A., and Matarrese, P. (2018) Cell death-based treatments of melanoma:conventional treatments and new therapeutic strategies. *Cell Death Dis.* **9**, 112
5. Gray-Schopfer, V. C., Cheong, S. C., Chong, H., Chow, J., Moss, T., Abdel-Malek, Z. A., Marais, R., Wynford-Thomas, D., and Bennett, D. C. (2006) Cellular senescence in naevi and immortalisation in melanoma: a role for p16? *Br. J. Cancer* **95**, 496–505
6. Scott, M. C., Wakamatsu, K., Ito, S., Kadekaro, A. L., Kobayashi, N., Groden, J., Kavanagh, R., Takakuwa, T., Virador, V., Hearing, V. J., and Abdel-Malek, Z. A. (2002) Human melanocortin 1 receptor variants, receptor function and melanocyte response to UV radiation. *J. Cell Sci.* **115**, 2349–2355
7. Jordan, M., Schallhorn, A., and Wurm, F. M. (1996) Transfecting mammalian cells: optimization of critical parameters affecting calcium-phosphate precipitate formation. *Nucleic Acids Res.* **24**, 596–601
8. Berggren, W. T., Lutz, M., and Modesto, V. (2008) *General Spinfection Protocol*, StemBook, Cambridge, MA, USA
9. Li, W., Xu, H., Xiao, T., Cong, L., Love, M. I., Zhang, F., Irizarry, R. A., Liu, J. S., Brown, M., and Liu, X. S. (2014) MAGeCK enables robust identification of essential genes from genome-scale CRISPR/Cas9 knockout screens. *Genome Biol.* **15**, 554
10. Sanjana, N. E., Shalem, O., and Zhang, F. (2014) Improved vectors and genome-wide libraries for CRISPR screening. *Nat. Methods* **11**, 783–784
11. Li, W., Köster, J., Xu, H., Chen, C. H., Xiao, T., Liu, J. S., Brown, M., and Liu, X. S. (2015) Quality control, modeling, and visualization of CRISPR screens with MAGeCK-VISPR. *Genome Biol.* **16**, 281
12. Rocha, C. R. R., Silva, M. M., Quinet, A., Cabral-Neto, J. B., and Menck, C. F. M. (2018) DNA repair pathways and cisplatin resistance: an intimate relationship. *Clinics (São Paulo)* **73** (Suppl 1), e478s
13. Hao, H. X., Xie, Y., Zhang, Y., Charlat, O., Oster, E., Avello, M., Lei, H., Mickanin, C., Liu, D., Ruffner, H., Mao, X., Ma, Q., Zamponi, R., Bouwmeester, T., Finan, P. M., Kirschner, M. W., Porter, J. A., Serluca, F. C., and Cong, F. (2012) ZNRF3 promotes Wnt receptor turnover in an R-spondin-sensitive manner. *Nature* **485**, 195–200
14. Huang, D. T., Ayrault, O., Hunt, H. W., Taherbhoy, A. M., Duda, D. M., Scott, D. C., Borg, L. A., Neale, G., Murray, P. J., Roussel, M. F., and Schulman, B. A. (2009) E2-RING expansion of the NEDD8 cascade confers specificity to cullin modification. *Mol. Cell* **33**, 483–495
15. Nusse, R., and Clevers, H. (2017) Wnt/β-catenin signaling, disease, and emerging therapeutic modalities. *Cell* **169**, 985–999

16. Zhan, T., Rindtorff, N., and Boutros, M. (2017) Wnt signaling in cancer. *Oncogene* **36**, 1461–1473
17. Niehrs, C., and Acebron, S. P. (2012) Mitotic and mitogenic Wnt signalling. *EMBO J.* **31**, 2705–2713
18. Koo, B. K., Spit, M., Jordens, I., Low, T. Y., Stange, D. E., van de Wetering, M., van Es, J. H., Mohammed, S., Heck, A. J., Maurice, M. M., and Clevers, H. (2012) Tumour suppressor RNF43 is a stem-cell E3 ligase that induces endocytosis of Wnt receptors. *Nature* **488**, 665–669
19. Ehmer, U., and Sage, J. (2016) Control of proliferation and cancer growth by the Hippo signaling pathway. *Mol. Cancer Res.* **14**, 127–140
20. Petrilli, A. M., and Fernández-Valle, C. (2016) Role of Merlin/NF2 inactivation in tumor biology. *Oncogene* **35**, 537–548
21. Morita, M., Ler, L. W., Fabian, M. R., Siddiqui, N., Mullin, M., Henderson, V. C., Alain, T., Fonseca, B. D., Karashchuk, G., Bennett, C. F., Kabuta, T., Higashi, S., Larsson, O., Topisirovic, I., Smith, R. J., Gingras, A. C., and Sonenberg, N. (2012) A novel 4EHP-GIGYF2 translational repressor complex is essential for mammalian development. *Mol. Cell. Biol.* **32**, 3585–3593
22. Von Stechow, L., Typas, D., Carreras Puigvert, J., Oort, L., Siddappa, R., Pines, A., Vrieling, H., van de Water, B., Mullenders, L. H., and Danen, E. H. (2015) The E3 ubiquitin ligase ARIH1 protects against genotoxic stress by initiating a 4EHP-mediated mRNA translation arrest. *Mol. Cell. Biol.* **35**, 1254–1268
23. Liu-Chittenden, Y., Huang, B., Shim, J. S., Chen, Q., Lee, S. J., Anders, R. A., Liu, J. O., and Pan, D. (2012) Genetic and pharmacological disruption of the TEAD-YAP complex suppresses the oncogenic activity of YAP. *Genes Dev.* **26**, 1300–1305
24. Song, S., Xie, M., Scott, A. W., Jin, J., Ma, L., Dong, X., Skinner, H. D., Johnson, R. L., Ding, S., and Ajani, J. A. (2018) A novel YAP1 inhibitor targets CSC-enriched radiation-resistant cells and exerts strong antitumor activity in esophageal adenocarcinoma. *Mol. Cancer Ther.* **17**, 443–454
25. Lasfargues, C., Martineau, Y., Bousquet, C., and Pyronnet, S. (2012) Changes in translational control after pro-apoptotic stress. *Int. J. Mol. Sci.* **14**, 177–190
26. Liu, B., and Qian, S. B. (2014) Translational reprogramming in cellular stress response. *Wiley Interdiscip. Rev. RNA* **5**, 301–315
27. Roesch, A., Vultur, A., Bogeski, I., Wang, H., Zimmermann, K. M., Speicher, D., Körbel, C., Laschke, M. W., Gimotty, P. A., Philipp, S. E., Krause, E., Pätzold, S., Villanueva, J., Krepler, C., Fukunaga-Kalabis, M., Hoth, M., Bastian, B. C., Vogt, T., and Herlyn, M. (2013) Overcoming intrinsic multidrug resistance in melanoma by blocking the mitochondrial respiratory chain of slow-cycling JARID1B(high) cells. *Cancer Cell* **23**, 811–825
28. Ma, L., Wang, R., Duan, H., Nan, Y., Wang, Q., and Jin, F. (2015) Mitochondrial dysfunction rather than mtDNA sequence mutation is responsible for the multi-drug resistance of small cell lung cancer. *Oncol. Rep.* **34**, 3238–3246
29. Wang, S. F., Chen, M. S., Chou, Y. C., Ueng, Y. F., Yin, P. H., Yeh, T. S., and Lee, H. C. (2016) Mitochondrial dysfunction enhances cisplatin resistance in human gastric cancer cells via the ROS-activated GCN2-eIF2α-ATF4-xCT pathway. *Oncotarget* **7**, 74132–74151
30. Thomas, M. P., Liu, X., Whangbo, J., McCrossan, G., Sanborn, K. B., Basar, E., Walch, M., and Lieberman, J. (2015) Apoptosis triggers specific, rapid, and global mRNA decay with 3′ uridylated intermediates degraded by DIS3L2. *Cell Rep.* **11**, 1079–1089
31. Fulda, S. (2014) Molecular pathways: targeting inhibitor of apoptosis proteins in cancer–from molecular mechanism to therapeutic application. *Clin. Cancer Res.* **20**, 289–295
32. Gupta, I., Singh, K., Varshney, N. K., and Khan, S. (2018) Delineating crosstalk mechanisms of the ubiquitin proteasome system that regulate apoptosis. *Front. Cell Dev. Biol.* **6**, 11
33. Stintzing, S., and Lenz, H. J. (2014) Molecular pathways: turning proteasomal protein degradation into a unique treatment approach. *Clin. Cancer Res.* **20**, 3064–3070
34. Mezencev, R. (2015) Interactions of cisplatin with non-DNA targets and their influence on anticancer activity and drug toxicity: the complex world of the platinum complex. *Curr. Cancer Drug Targets* **14**, 794–816
35. Kastenhuber, E. R., and Lowe, S. W. (2017) Putting p53 in context. *Cell* **170**, 1062–1078
36. Tang, C. H., and Grimm, E. A. (2004) Depletion of endogenous nitric oxide enhances cisplatin-induced apoptosis in a p53-dependent manner in melanoma cell lines. *J. Biol. Chem.* **279**, 288–298
37. Hamaratoglu, F., Willecke, M., Kango-Singh, M., Nolo, R., Hyun, E., Tao, C., Jafar-Nejad, H., and Halder, G. (2006) The tumour-suppressor genes NF2/Merlin and expanded act through Hippo signalling to regulate cell proliferation and apoptosis. *Nat. Cell Biol.* **8**, 27–36; erratum: 100
38. Dalal, S., Connelly, B. A., Singh, M., and Singh, K. (2017) Involvement of NF2 signaling pathway in β-adrenergic receptor-stimulated cardiac myocyte apoptosis. *FASEB J.* **31** (suppl 1), 876.7 (abstr.)
39. Yuan, T., Gorrepati, K. D., Maedler, K., and Ardestani, A. (2016) Loss of Merlin/NF2 protects pancreatic β-cells from apoptosis by inhibiting LATS2. *Cell Death Dis.* **7**, e2107
40. Huang, J. M., Nagatomo, I., Suzuki, E., Mizuno, T., Kumagai, T., Berezov, A., Zhang, H., Karlan, B., Greene, M. I., and Wang, Q. (2013) YAP modifies cancer cell sensitivity to EGFR and survivin inhibitors and is negatively regulated by the non-receptor type protein tyrosine phosphatase 14. *Oncogene* **32**, 2220–2229
41. Overholtzer, M., Zhang, J., Smolen, G. A., Muir, B., Li, W., Sgroi, D. C., Deng, C. X., Brugge, J. S., and Haber, D. A. (2006) Transforming properties of YAP, a candidate oncogene on the chromosome 11q22 amplicon. *Proc. Natl. Acad. Sci. USA* **103**, 12405–12410
42. Xia, Y., Chang, T., Wang, Y., Liu, Y., Li, W., Li, M., and Fan, H. Y. (2014) YAP promotes ovarian cancer cell tumorigenesis and is indicative of a poor prognosis for ovarian cancer patients. *PLoS One* **9**, e91770; erratum: 11, e0152712
43. Zhang, X., George, J., Deb, S., Degoutin, J. L., Takano, E. A., Fox, S. B., Bowtell, D. D., and Harvey, K. F.; AOCS Study group. (2011) The Hippo pathway transcriptional co-activator, YAP, is an ovarian cancer oncogene. *Oncogene* **30**, 2810–2822
44. Ren, A., Yan, G., You, B., and Sun, J. (2008) Down-regulation of mammalian sterile 20-like kinase 1 by heat shock protein 70 mediates cisplatin resistance in prostate cancer cells. *Cancer Res.* **68**, 2266–2274
45. Villa, E., Proïcs, E., Rubio-Patiño, C., Obba, S., Zunino, B., Bossowski, J. P., Rozier, R. M., Chiche, J., Mondragón, L., Riley, J. S., Marchetti, S., Verhoeyen, E., Tait, S. W. G., and Ricci, J. E. (2017) Parkin-independent mitophagy controls chemotherapeutic response in cancer cells. *Cell Rep.* **20**, 2846–2859

Received for publication July 25, 2018.
Accepted for publication February 18, 2019.

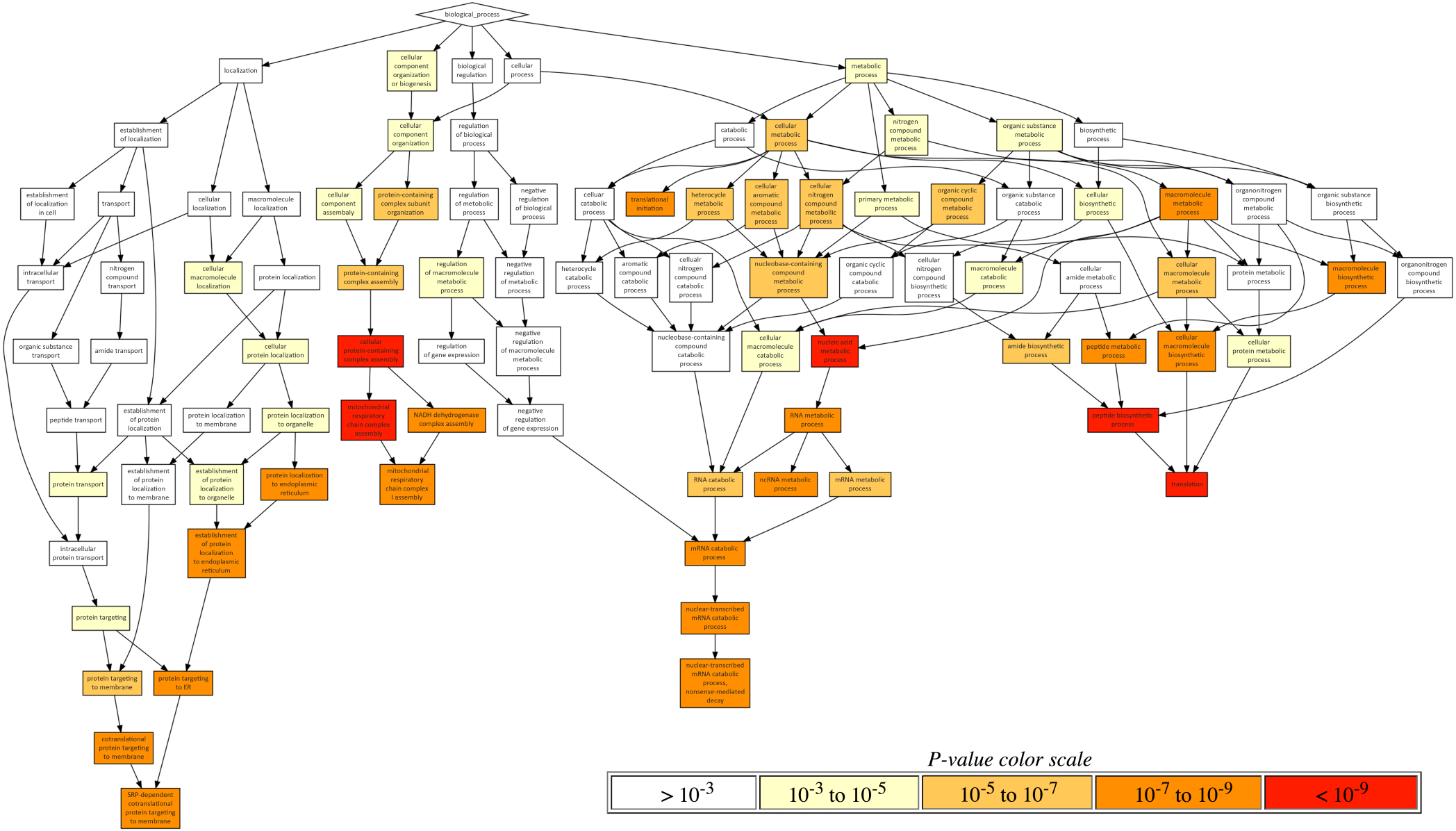

Supplementary Fig. S1. Top disrupted biological processes positively selected by cisplatin in A375 human melanoma cells.

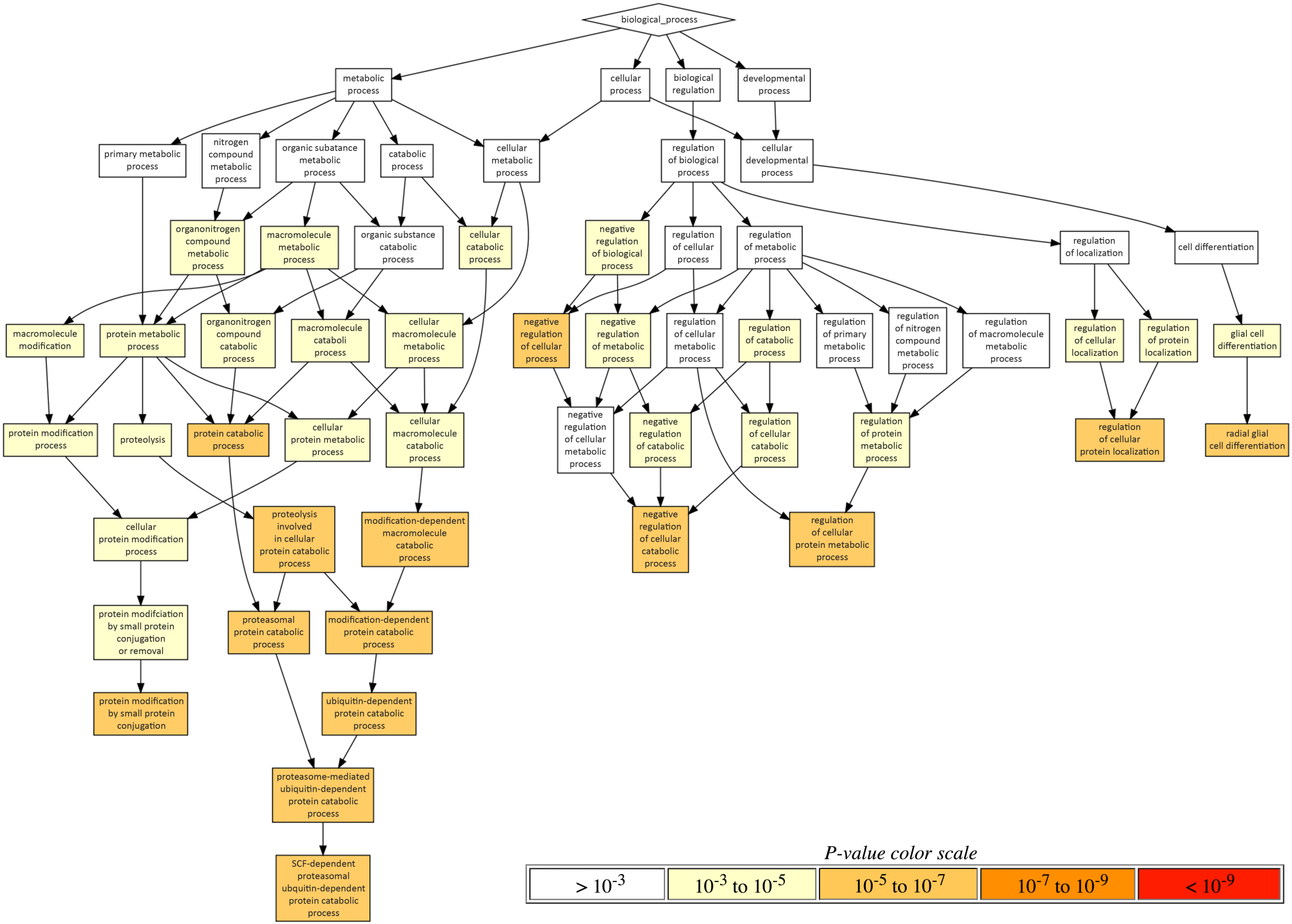

Supplementary Fig. S2. Top disrupted biological processes negatively selected by cisplatin in A375 human melanoma cells.

Supplementary Table S1. Oligonucleotides used for sequencing of GeCKO sgRNAs.	
Lenti-F1	ATGGACTATCATATGCTTACCGTAACTTGAAAGTATTTCG
Lenti-R1	ACTTCTTGTCCATGGTGGCAGC
GECKO1	ACACGACGCTCTTCCGATCTTCTTGTGGAAAGGACGAAACACCG
GECKO2-2	AGACGTGTGCTCTTCCGATCTCACTTTTTCAAGTTGATAACGGACTAGCC
Tru-U	AATGATACGGCGACCACCGAGATCTACACTCTTTCCCTACACGACGCTCTTCCGATCT
Tru-B1	CAAGCAGAAGACGGCATACGAGATCGTGATGTGACTGGAGTTCAGACGTGTGCTCTTCCGATCT
Tru-B2	CAAGCAGAAGACGGCATACGAGATACATCGGTGACTGGAGTTCAGACGTGTGCTCTTCCGATCT
Tru-B3	CAAGCAGAAGACGGCATACGAGATGCCTAAGTGACTGGAGTTCAGACGTGTGCTCTTCCGATCT

Supplementary Table S2. Knockdown efficiencies of shRNA-encoding sequences[a].				
shRNA	**Sequence**	**A375**	**Hermes 4C**	**P1F/TERT**
shNF2-1	CCGGTACTTTGCAATCCGGAATAAACTCGAGTTTATTCCGGATTGCAAAGTATTTTTG	good	N/T	poor
shNF2-2	CCGGTCGGGAACCATGATCTATTTACTCGAGTAAATAGATCATGGTTCCCGATTTTTG	good	good	good
shNF2-3	CCGGCTGTGTTGTCCACCCTATTATCTCGAGATAATAGGGTGGACAACACAGTTTTTG	poor	N/T	average
shNF2-4	CCGGTAGTTCTCTGACCTGAGTCTTCTCGAGAAGACTCAGGTCAGAGAACTATTTTTG	good	N/T	good
shRNF7-1	CCGGTCAGAAATTCTCTGCGATTAACTCGAGTTAATCGCAGAGAATTTCTGATTTTTG	good	good	good
shRNF7-2	CCGGTGCTTATGGTTGATCAGTTAACTCGAGTTAACTGATCAACCATAAGCATTTTTG	good	N/T	good
shRNF7-3	CCGGCCCAACTCTTACTCTTAATTTCTCGAGAAATTAAGAGTAAGAGTTGGGTTTTTG	average	good	poor
shRNF7-4	CCGGACAGCTTAGAAGTGCTATAAACTCGAGTTTATAGCACTTCTAAGCTGTTTTTTG	N/T	N/T	poor
shUBE2F-1	CCGGGATGACTACATCAAACGTTATCTCGAGATAACGTTTGATGTAGTCATCTTTTTTG	good	N/T	N/T
shUBE2F-2	CCGGGCAATAAGATACCCGCTACAACTCGAGTTGTAGCGGGTATCTTATTGCTTTTTG	poor	poor	N/T
shUBE2F-3	CCGGTTCTGCACAAGCGATGCTAATCTCGAGATTAGCATCGCTTGTGCAGAATTTTTTG	poor	good	N/T
shUBE2F-4	CCGGTGATCCAAACAAGCTTCATTGCTCGAGCAATGAAGCTTGTTTGGATCATTTTTTG	good	good	N/T
shZNRF3-1	CCGGGTCTACCTAATGCACTATTATCTCGAGATAATAGTGCATTAGGTAGACTTTTTG	good	good	poor
shZNRF3-2	CCGGTCCTCGACAACCCACTGAATACTCGAGTATTCAGTGGGTTGTCGAGGATTTTTG	poor	N/T	poor
shZNRF3-3	CCGGGAAGGGTGCAGATGCCATTAACTCGAGTTAATGGCATCTGCACCCTTCTTTTTG	good	N/T	poor
shZNRF3-4	CCGGACTGTCGGCACAACATCATAGCTCGAGCTATGATGTTGTGCCGACAGTTTTTTG	good	poor	poor
shCTNNB1-1	CCGGATCTGTCTGCTCTAGTAATAACTCGAGTTATTACTAGAGCAGACAGATTTTTTG	poor	poor	N/T
shCTNNB1-2	CCGGGGGAGTGGTTTAGGCTATTTGCTCGAGCAAATAGCCTAAACCACTCCCTTTTTG	poor	N/T	N/T
shCTNNB1-3	CCGGTCTAACCTCACTTGCAATAATCTCGAGATTATTGCAAGTGAGGTTAGATTTTTG	good	good	N/T
shCTNNB1-4	CCGGTTGTTATCAGAGGACTAAATACTCGAGTATTTAGTCCTCTGATAACAATTTTTG	average	poor	N/T
shTP53	CCGGCACCATCCACTACAACTACATCTCGAGATGTAGTTGTAGTGGATGGTGTTTTTG	good	N/T	N/T
Scramble	CCGGTCCTAAGGTTAAGTCGCCCTCGCTCGAGCGAGGGCGACTTAACCTTAGGTTTTTG	control	control	control

[a] 'good', 'average' and 'poor' refer to > 80, 50-80 and < 50% knockdowns, respectively. N/T, not tested.

Supplementary Table S3. Reverse transcription and quantitative PCR primers.		
Primers for reverse transcription		
ACTB	AGCAATGATCTTGAT	
ARIH1	CTCACAGTATCTG	
EIF4E2	TGTCTTCCTGAAAGC	
Primers for real-time quantitative PCR of cDNAs		
ACTB	CTTCCTGGGCATGGAGTCC	AGCAATGATCTTGATCTTCATTGTGCTG
ARIH1	CCATTATCTTTGAGAATAACCAAGCAGATC	TCTCACAGTATCTGTACTTGTCTTGTACTTTCTG
EIF4E2	CCCATGTGGGAGGATGATGC	TGTCTTCCTGAAAGCGGACAGAC

Supplementary Table S4. Top disrupted genes positively selected by cisplatin in A375 cells[a].

Gene	sgRNA #	Score	p-value	FDR	Rank	Good sgRNA	LFC
ST13	6	7.55E-07	2.51E-06	0.03713	1	3	1.9456
hsa-mir-5787	4	2.16E-06	3.42E-06	0.03713	2	3	2.4981
HIST2H2BE	6	5.45E-06	2.35E-05	0.12970	3	4	2.0374
ISCU	6	6.77E-06	2.99E-05	0.12970	4	3	1.9083
hsa-mir-548i-3	2	1.29E-05	2.85E-05	0.12970	5	2	3.5884
LOC200726	6	2.51E-05	8.10E-05	0.25106	6	1	0.3140
SOX10	6	2.53E-05	8.10E-05	0.25106	7	3	1.7642

[a] Genes with an FDR (false discovery rate) < 0.3 are listed. LFC, $\log_2$ fold change.

Supplementary Table S5. Top disrupted genes negatively selected by cisplatin in A375 cells[a].

Gene	sgRNA #	Score	p-value	FDR	Rank	Good sgRNA	LFC
RNF7	6	3.32E-13	2.28E-07	0.00099	1	6	-4.2083
ZNRF3	6	1.96E-10	2.28E-07	0.00099	2	6	-3.5136
UBE2F	6	9.10E-10	2.28E-07	0.00099	3	5	-3.6303
CUL5	6	1.13E-08	2.28E-07	0.00099	4	6	-3.7347
JUNB	6	2.65E-08	2.28E-07	0.00099	5	6	-2.4162
CUL3	6	8.28E-08	6.84E-07	0.0025	6	6	-3.0936
HES1	6	4.79E-07	2.97E-06	0.0092	7	6	-2.5041
AMBRA1	6	2.42E-06	1.21E-05	0.0328	8	6	-2.1830
SLC26A4	6	3.26E-06	1.51E-05	0.0363	9	5	-2.2510
TAOK1	6	5.00E-06	2.81E-05	0.0581	10	6	-1.3644
OR5D14	6	5.27E-06	2.94E-05	0.0581	11	6	-1.4396
SRGAP2B	6	1.20E-05	7.42E-05	0.1238	12	6	-1.4222
ARRDC3	6	1.78E-05	0.00010	0.1541	13	6	-1.8967
PTPN14	6	1.83E-05	0.00011	0.1541	14	6	-1.7067
MAPK14	6	2.31E-05	0.00014	0.1847	15	6	-1.2357
KDM4A	6	2.51E-05	0.00015	0.1867	16	3	-0.0053
RPL11	6	4.05E-05	0.00023	0.2602	17	3	-0.1948
STAT3	6	4.33E-05	0.00024	0.2602	18	4	-1.7606
WAPAL	6	4.56E-05	0.00025	0.2602	19	5	-1.6982
PHF23	6	4.70E-05	0.00026	0.2602	20	6	-1.5824
PHF21A	6	5.01E-05	0.00027	0.2602	21	5	-1.6883
NF2	6	5.05E-05	0.00028	0.2602	22	4	-1.1018
DGKD	6	5.58E-05	0.00030	0.2708	23	6	-1.1621
TBC1D3H	1	6.28E-05	0.00007	0.1176	24	1	-7.0302

[a] Genes with an FDR (false discovery rate) < 0.3 are listed. LFC, $\log_2$ fold change.

Supplementary Table S6. Top disrupted genes causing decreased fitness for A375 cells[a].

Gene	sgRNA #	Score	p-value	FDR	Rank	Good sgRNA	LFC
MAD2L1	6	1.00E-11	2.28E-07	0.00050	1	6	-4.3154
SOX10	6	1.05E-09	2.28E-07	0.00050	2	6	-3.3105
hsa-mir-8086	4	3.27E-09	2.28E-07	0.00050	3	4	-5.1739
hsa-mir-1299	4	3.38E-09	2.28E-07	0.00050	4	4	-4.3318
DUX2	6	8.05E-09	2.28E-07	0.00050	5	6	-2.9258

RPL3	6	4.07E-08	2.28E-07	0.00050	6	6	-3.3296
hsa-mir-3929	4	7.05E-08	2.28E-07	0.00050	7	4	-4.3375
hsa-mir-6859-1	4	1.20E-07	2.28E-07	0.00050	8	4	-3.127
RPS27	6	1.31E-07	6.84E-07	0.00135	9	5	-3.2276
hsa-mir-6087	4	1.83E-07	2.28E-07	0.00050	10	4	-4.8855
HAUS3	6	1.83E-07	1.14E-06	0.00177	11	6	-2.6301
RPL23A	6	2.32E-07	1.14E-06	0.00177	12	5	-3.2757
RPLP0	6	2.34E-07	1.14E-06	0.00177	13	6	-2.7929
SPDYE5	4	2.64E-07	2.28E-07	0.00050	14	4	-2.8423
AGAP4	6	3.39E-07	1.60E-06	0.00204	15	6	-1.8938
PDCD2	6	3.42E-07	1.60E-06	0.00204	16	6	-2.541
PSMB3	6	3.86E-07	1.60E-06	0.00204	17	6	-2.4105
PHB2	6	4.04E-07	2.05E-06	0.00248	18	5	-3.2318
TPI1	6	4.43E-07	2.51E-06	0.00287	19	6	-2.411
RPL13	6	5.70E-07	2.97E-06	0.00322	20	6	-3.08
NDUFB10	6	6.54E-07	3.42E-06	0.00323	21	6	-2.2572
KATNB1	6	7.18E-07	3.42E-06	0.00323	22	5	-2.1404
CPSF4	6	7.53E-07	3.42E-06	0.00323	23	6	-3.2095
SRSF1	6	8.35E-07	3.88E-06	0.00337	24	6	-2.3581
TRMT112	6	1.17E-06	6.62E-06	0.00532	25	6	-3.0153
hsa-mir-1207	4	1.44E-06	3.88E-06	0.00337	26	4	-4.138
CAD	6	1.65E-06	9.35E-06	0.00687	27	6	-2.877
hsa-mir-6511a-4	4	1.67E-06	4.34E-06	0.00362	28	4	-2.2701
GAPDH	6	1.69E-06	9.35E-06	0.00687	29	5	-2.8177
GNB2L1	6	1.79E-06	9.81E-06	0.00687	30	6	-2.4251
RPL34	6	1.85E-06	1.07E-05	0.00705	31	6	-2.8123
WASH1	6	1.99E-06	1.12E-05	0.00714	32	6	-2.5943
NBPF1	6	2.43E-06	1.21E-05	0.00750	33	5	-2.1046
CCNA2	6	2.69E-06	1.28E-05	0.00770	34	6	-2.3619
hsa-mir-663a	4	2.87E-06	9.81E-06	0.00687	35	4	-3.1129
POLR2D	6	2.95E-06	1.44E-05	0.00800	36	6	-2.6186
hsa-mir-8078	4	2.95E-06	1.07E-05	0.00705	37	4	-3.5425
PCNA	6	2.97E-06	1.44E-05	0.00800	38	5	-2.2495
ELP3	6	2.97E-06	1.44E-05	0.00800	39	6	-1.8302
NIP7	6	3.44E-06	1.67E-05	0.00904	40	6	-2.2995
COPA	6	3.85E-06	1.80E-05	0.00931	41	6	-2.5604
LIPT1	6	4.40E-06	2.35E-05	0.01127	42	6	-2.0815
RPL13A	6	4.44E-06	2.40E-05	0.01127	43	6	-1.4916
MRPL3	6	4.54E-06	2.44E-05	0.01127	44	6	-1.8421
RPS15A	6	4.83E-06	2.72E-05	0.01202	45	5	-2.6826
hsa-mir-5096	4	5.02E-06	1.71E-05	0.00906	46	4	-4.4355
hsa-mir-1273a	4	5.49E-06	1.89E-05	0.00956	47	4	-3.9641
RPL4	6	5.98E-06	3.35E-05	0.01455	48	6	-2.6182
TBCA	6	6.57E-06	3.90E-05	0.01628	49	5	-3.0493
POLR3K	6	7.10E-06	4.40E-05	0.01803	50	6	-1.5762
hsa-mir-7641-1	4	7.25E-06	2.35E-05	0.01127	51	4	-3.352
POLR3H	6	7.56E-06	4.63E-05	0.01845	52	4	-2.9996
POLR2E	6	7.71E-06	4.68E-05	0.01845	53	6	-2.2638
hsa-mir-566	4	8.46E-06	2.72E-05	0.01202	54	4	-3.4877
NELFB	6	8.54E-06	5.23E-05	0.02024	55	5	-1.6621
RPS28	6	9.28E-06	5.68E-05	0.02163	56	6	-2.2783
ST13	6	1.00E-05	6.05E-05	0.02262	57	5	-2.9632
CBWD1	4	1.07E-05	3.45E-05	0.01466	58	4	-2.2694
POLR3A	6	1.13E-05	7.05E-05	0.02538	59	6	-1.8625
PSMG1	6	1.14E-05	7.19E-05	0.02538	60	5	-1.7905
PSMA6	6	1.19E-05	7.37E-05	0.02538	61	6	-2.1558
RPL24	6	1.19E-05	7.37E-05	0.02538	62	4	-2.6417
ISCA2	6	1.28E-05	7.94E-05	0.02658	63	6	-2.1943
KPNB1	6	1.29E-05	7.96E-05	0.02658	64	6	-1.5808
PSMG4	6	1.37E-05	8.42E-05	0.02727	65	4	-2.6344
RABGGTB	6	1.40E-05	8.69E-05	0.02774	66	6	-2.397
ATP6V0C	6	1.55E-05	9.20E-05	0.02891	67	6	-2.3224

RPL30	6	1.67E-05	9.79E-05	0.02991	68	6	-2.3889
ALG14	6	1.68E-05	9.83E-05	0.02991	69	6	-1.5548
POP5	6	1.68E-05	9.93E-05	0.02991	70	5	-2.5976
RPA3	6	1.79E-05	0.00010	0.03086	71	4	-2.5047
VPS28	6	1.83E-05	0.00011	0.03094	72	5	-2.2318
FDX1L	6	1.85E-05	0.00011	0.03094	73	6	-1.9749
hsa-mir-663b	4	2.05E-05	0.00007	0.02538	74	4	-3.3695
SRSF7	6	2.07E-05	0.00012	0.03414	75	5	-1.923
SNRPD1	6	2.15E-05	0.00013	0.03510	76	6	-1.9019
GINS1	6	2.26E-05	0.00013	0.03620	77	5	-2.522
BUD31	6	2.35E-05	0.00014	0.03632	78	5	-2.2966
SNRPD3	6	2.36E-05	0.00014	0.03632	79	6	-2.1878
SUPT6H	6	2.39E-05	0.00014	0.03632	80	6	-1.2925
ELP5	6	2.44E-05	0.00014	0.03632	81	4	-2.1629
NRF1	6	2.46E-05	0.00014	0.03632	82	6	-1.9883
NCMAP	6	2.51E-05	0.00015	0.03632	83	3	0.10308
RPS11	6	2.59E-05	0.00015	0.03632	84	5	-2.3683
ALG11	6	2.61E-05	0.00015	0.03632	85	4	-2.7084
UFD1L	6	2.78E-05	0.00016	0.03801	86	6	-1.7139
hsa-mir-4516	4	3.01E-05	0.00011	0.03094	87	4	-2.2298
SMC6	6	3.05E-05	0.00017	0.04111	88	6	-2.1526
TOMM20	6	3.05E-05	0.00017	0.04111	89	5	-1.9876
MYC	6	3.22E-05	0.00018	0.04306	90	6	-1.497
NSMCE1	6	3.25E-05	0.00019	0.04313	91	6	-1.3573
TP53TG3	5	3.31E-05	0.00014	0.03632	92	5	-1.204
NFS1	6	3.33E-05	0.00019	0.04372	93	4	-2.0648
RPL17	6	3.67E-05	0.00021	0.04718	94	5	-2.0727
hsa-mir-3180-4	4	3.71E-05	0.00013	0.03616	95	4	-1.8653
RPL38	6	3.75E-05	0.00021	0.04733	96	5	-1.7908
LSM2	6	3.76E-05	0.00021	0.04733	97	6	-1.9897
EIF2B2	6	3.93E-05	0.00022	0.04926	98	6	-1.47
TBC1D3F	2	3.95E-05	0.00008	0.02678	99	2	-4.1909
SF3B1	6	4.06E-05	0.00023	0.04973	100	6	-1.6609
RPL32	6	4.08E-05	0.00023	0.04973	101	5	-2.1005
RPL14	6	4.20E-05	0.00024	0.04973	102	5	-2.2444
GTF2E2	6	4.24E-05	0.00024	0.04973	103	5	-1.9915
RPL37A	6	4.31E-05	0.00024	0.04973	104	6	-1.1992
YARS	6	4.36E-05	0.00024	0.04973	105	4	-2.0783
EIF5AL1	6	4.47E-05	0.00025	0.04973	106	4	-2.3921
TSR1	6	4.48E-05	0.00025	0.04973	107	6	-1.5705
ANAPC5	6	4.50E-05	0.00025	0.04973	108	5	-2.4837
HIST2H2BE	6	4.71E-05	0.00026	0.05144	109	5	-2.1599
PRPF38A	6	5.03E-05	0.00027	0.05288	110	5	-1.9487
GTF2H5	6	5.04E-05	0.00027	0.05288	111	5	-1.4541
LOC100507462	6	5.04E-05	0.00028	0.05288	112	4	-1.0652
NOP58	6	5.20E-05	0.00028	0.05332	113	5	-2.1996
MTHFD1	6	5.31E-05	0.00029	0.05332	114	5	-1.222
RPL18A	6	5.37E-05	0.00029	0.05332	115	6	-1.865
RPS20	6	5.40E-05	0.00029	0.05332	116	4	-2.2599
SNRPF	6	5.57E-05	0.00030	0.05332	117	6	-2.0452
MED8	6	5.63E-05	0.00030	0.05332	118	5	-1.9986
PES1	6	5.65E-05	0.00030	0.05332	119	6	-2.0876
POLR2I	6	5.68E-05	0.00031	0.05332	120	6	-2.1453
RPP38	6	5.69E-05	0.00031	0.05332	121	6	-1.5354
RBMX	6	5.70E-05	0.00031	0.05332	122	5	-1.5166
TOMM22	6	5.70E-05	0.00031	0.05332	123	5	-2.0332
MARS2	6	5.73E-05	0.00031	0.05332	124	6	-2.084
SPC24	6	5.81E-05	0.00031	0.05336	125	5	-1.7853
SRSF3	6	5.95E-05	0.00032	0.05372	126	6	-2.3208
ATP6V1B2	6	6.02E-05	0.00032	0.05384	127	6	-1.0294
GINS4	6	6.12E-05	0.00032	0.05396	128	5	-1.8882
MRPL36	6	6.19E-05	0.00033	0.05483	129	6	-1.6052

ISCU	6	6.29E-05	0.00033	0.05490	130	5	-2.0482
MAD2L2	6	6.32E-05	0.00034	0.05490	131	3	-1.4164
RPL10	6	6.38E-05	0.00034	0.05501	132	5	-1.8096
CDC20	6	6.44E-05	0.00034	0.05518	133	6	-2.0397
NLE1	6	6.50E-05	0.00035	0.05518	134	4	-1.9696
PCGF1	6	6.51E-05	0.00035	0.05518	135	6	-1.9687
hsa-mir-1273d	4	6.52E-05	0.00024	0.04973	136	4	-2.822
GPX4	6	6.66E-05	0.00036	0.05579	137	6	-1.2887
CEP97	6	6.69E-05	0.00036	0.05579	138	5	-1.8927
ASH2L	6	6.77E-05	0.00036	0.05579	139	5	-1.9073
RPS24	6	6.79E-05	0.00036	0.05579	140	6	-2.1653
EED	6	7.13E-05	0.00039	0.05814	141	6	-1.931
PKD1	6	7.14E-05	0.00039	0.05814	142	3	-1.4668
ACTG1	6	7.16E-05	0.00039	0.05814	143	5	-2.1988
RPL21	6	7.19E-05	0.00039	0.05814	144	5	-2.2099
VPS25	6	7.47E-05	0.00040	0.05883	145	5	-1.9582
PROX2	6	7.53E-05	0.00040	0.05884	146	4	-0.087384
BARD1	6	7.63E-05	0.00040	0.05885	147	6	-1.8979
EMC6	6	7.68E-05	0.00041	0.05885	148	6	-1.691
DUT	6	7.97E-05	0.00042	0.06061	149	5	-2.3518
NDUFB9	6	8.34E-05	0.00045	0.06319	150	5	-1.099
EIF3J	6	8.60E-05	0.00046	0.06529	151	6	-1.8885
NXNL2	6	8.82E-05	0.00048	0.06693	152	4	-1.8703
POLR2L	6	8.89E-05	0.00048	0.06693	153	4	-1.641
NBPF9	5	9.04E-05	0.00041	0.05931	154	4	-1.9872
RBM14	6	9.17E-05	0.00049	0.06820	155	4	-2.672
ZNRD1	6	9.26E-05	0.00050	0.06859	156	5	-2.2323
PHAX	6	9.70E-05	0.00053	0.07239	157	6	-0.96924
RPS5	6	9.82E-05	0.00054	0.07245	158	4	-2.0616
RFC5	6	9.82E-05	0.00054	0.07245	159	6	-0.8258
SDHD	6	9.86E-05	0.00054	0.07245	160	6	-2.0779
POP7	6	0.00010	0.00055	0.07302	161	5	-1.9984
SNRPC	4	0.00010	0.00039	0.05869	162	4	-1.4432
EIF3I	6	0.00010	0.00056	0.07402	163	5	-1.8175
NOC4L	6	0.00010	0.00057	0.07476	164	6	-1.9606
ARFRP1	6	0.00011	0.00058	0.07538	165	5	-1.4676
MRPL34	6	0.00011	0.00059	0.07659	166	6	-1.6714
CHEK1	6	0.00011	0.00061	0.07812	167	5	-1.9143
RPL23	6	0.00011	0.00062	0.07871	168	5	-2.2784
PSMD14	6	0.00011	0.00063	0.07895	169	6	-1.7397
WDR74	6	0.00011	0.00063	0.07895	170	6	-2.3644
METTL1	6	0.00012	0.00064	0.07981	171	6	-1.747
PTPMT1	6	0.00012	0.00064	0.07998	172	6	-1.9682
WDR44	6	0.00012	0.00065	0.08048	173	5	-1.33
SPANXF1	5	0.00012	0.00055	0.07302	174	3	-2.4949
DCLRE1C	6	0.00012	0.00067	0.08216	175	6	-0.96208
PPP2R4	6	0.00012	0.00068	0.08248	176	3	-1.3363
RPS16	6	0.00012	0.00068	0.08248	177	5	-2.0965
PCNT	6	0.00013	0.00068	0.08248	178	3	0.24763
SMARCA5	6	0.00013	0.00068	0.08248	179	6	-1.8062
PPP2CA	6	0.00013	0.00070	0.08315	180	5	-1.8937
SART3	6	0.00013	0.00070	0.08315	181	6	-1.9082
RPL11	6	0.00013	0.00071	0.08359	182	5	-2.2418
PPM1G	6	0.00013	0.00072	0.08448	183	6	-1.3468
RPL27A	6	0.00013	0.00073	0.08448	184	5	-1.6111
RIOK1	6	0.00013	0.00073	0.08448	185	6	-1.1755
NOP16	6	0.00014	0.00076	0.08803	186	5	-1.9293
PSMB4	6	0.00014	0.00078	0.08924	187	6	-2.2853
PSMB1	6	0.00014	0.00078	0.08924	188	5	-1.344
CDK2	6	0.00014	0.00079	0.08924	189	6	-1.4592
RPL7	6	0.00014	0.00079	0.08924	190	5	-2.2069
IMP4	6	0.00015	0.00081	0.09049	191	5	-1.302

SLC25A26	6	0.00015	0.00082	0.09049	192	5	-2.012
CASC5	6	0.00015	0.00082	0.09049	193	6	-1.2895
IARS	6	0.00015	0.00082	0.09049	194	6	-0.91107
MYBL2	6	0.00015	0.00083	0.09108	195	5	-1.1534
SRSF2	6	0.00016	0.00086	0.09232	196	6	-2.1529
RAD9A	6	0.00016	0.00086	0.09232	197	5	-1.7527
SRP54	6	0.00016	0.00086	0.09232	198	5	-1.953
hsa-mir-6859-2	2	0.00016	0.00031	0.05332	199	2	-3.7852
SAP130	6	0.00016	0.00088	0.09387	200	5	-1.2317
PDPK1	6	0.00016	0.00089	0.09387	201	4	-0.45719
DHX9	6	0.00016	0.00089	0.09387	202	5	-2.3682
HTRA2	6	0.00017	0.00090	0.09482	203	5	-1.8544
PSMB2	6	0.00017	0.00091	0.09482	204	6	-1.5706
PSTK	6	0.00017	0.00091	0.09482	205	6	-1.195
SNRPA1	6	0.00017	0.00091	0.09482	206	6	-1.2345
AK6	6	0.00017	0.00094	0.09624	207	5	-1.7631
MKI67IP	6	0.00017	0.00094	0.09624	208	4	-1.7887
TP53RK	6	0.00017	0.00094	0.09624	209	6	-2.3075
DOLPP1	6	0.00018	0.00096	0.09725	210	4	-0.22466
HUS1	6	0.00018	0.00097	0.09725	211	6	-1.7934
C10orf76	6	0.00018	0.00097	0.09725	212	5	-1.0794
OR4F16	5	0.00018	0.00085	0.09232	213	5	-1.0508
CDK11B	6	0.00019	0.00100	0.09930	214	5	-1.6289
CRCP	6	0.00019	0.00100	0.09930	215	5	-1.8089
hsa-mir-483	4	0.00019	0.00071	0.08359	216	4	-3.353

[a] Genes with an FDR (false discovery rate) < 0.1 are listed. LFC, $\log_2$ fold change.

Supplementary Table S7. Top disrupted biological processes positively selected by cisplatin in A375 cells[a].

GO id	GO term	p-value	FDR	Enrichment (B, n, b)
GO:0034622	cellular protein-containing complex assembly	2.74E-13	4.26E-09	1.42 (812,5297,334)
GO:0006412	translation	6.01E-13	4.67E-09	2.01 (194,4462,95)
GO:0043043	peptide biosynthetic process	1.50E-12	7.75E-09	1.76 (214,5837,120)
GO:0033108	mitochondrial respiratory chain complex assembly	2.38E-11	9.25E-08	2.26 (90,5320,59)
GO:0090304	nucleic acid metabolic process	1.94E-10	6.02E-07	1.20 (2184,5728,822)
GO:0072599	establishment of protein localization to endoplasmic reticulum	2.00E-09	5.17E-06	2.28 (107,4128,55)
GO:0009059	macromolecule biosynthetic process	2.05E-09	4.54E-06	1.26 (1260,5691,494)
GO:0034660	ncRNA metabolic process	2.21E-09	4.30E-06	1.39 (507,6326,243)
GO:0016070	RNA metabolic process	2.56E-09	4.43E-06	1.27 (1571,4557,497)
GO:0045047	protein targeting to ER	2.66E-09	4.14E-06	1.97 (103,5868,65)
GO:0070972	protein localization to endoplasmic reticulum	2.80E-09	3.96E-06	2.20 (119,4128,59)
GO:0006614	SRP-dependent cotranslational protein targeting to membrane	3.32E-09	4.30E-06	2.39 (89,4128,48)
GO:0034645	cellular macromolecule biosynthetic process	3.59E-09	4.29E-06	1.29 (999,5705,402)
GO:0006613	cotranslational protein targeting to membrane	1.02E-08	1.13E-05	2.31 (94,4128,49)
GO:0000184	nuclear-transcribed mRNA catabolic process, nonsense-mediated decay	2.02E-08	2.10E-05	2.08 (116,4472,59)
GO:0043170	macromolecule metabolic process	2.86E-08	2.78E-05	1.09 (5814,6326,2188)
GO:0000956	nuclear-transcribed mRNA catabolic process	3.00E-08	2.74E-05	1.83 (187,4165,78)
GO:0006518	peptide metabolic process	3.12E-08	2.69E-05	1.48 (336,5837,158)
GO:0010257	NADH dehydrogenase complex assembly	3.12E-08	2.55E-05	2.40 (58,4999,38)
GO:0032981	mitochondrial respiratory chain complex I assembly	3.12E-08	2.42E-05	2.40 (58,4999,38)
GO:0006402	mRNA catabolic process	3.18E-08	2.35E-05	1.80 (203,4165,83)
GO:0006413	translational initiation	6.11E-08	4.31E-05	1.96 (138,4128,61)
GO:0043604	amide biosynthetic process	1.12E-07	7.55E-05	1.60 (325,4155,118)
GO:0006139	nucleobase-containing compound metabolic process	2.01E-07	0.00013	1.14 (2724,6308,1068)
GO:0044237	cellular metabolic process	2.27E-07	0.00014	1.07 (7205,6318,2663)
GO:0046483	heterocycle metabolic process	2.80E-07	0.00017	1.13 (2885,6326,1128)
GO:0006401	RNA catabolic process	3.26E-07	0.00019	1.68 (232,4222,90)
GO:0043933	protein-containing complex subunit organization	3.30E-07	0.00018	1.18 (1771,6061,691)

GO:0016072	rRNA metabolic process	5.62E-07	0.00030	1.54 (219,5828,107)
GO:0006725	cellular aromatic compound metabolic process	6.40E-07	0.00033	1.13 (2931,6326,1141)
GO:0034470	ncRNA processing	6.53E-07	0.00033	1.40 (351,6284,168)
GO:0006396	RNA processing	1.13E-06	0.00055	1.26 (794,6287,342)
GO:0006364	rRNA processing	1.35E-06	0.00063	1.56 (192,5828,95)
GO:0034641	cellular nitrogen compound metabolic process	1.45E-06	0.00066	1.12 (3207,6308,1234)
GO:0044260	cellular macromolecule metabolic process	1.85E-06	0.00082	1.12 (4559,4244,1187)
GO:1901360	organic cyclic compound metabolic process	2.04E-06	0.00088	1.12 (3145,6308,1210)
GO:0016071	mRNA metabolic process	2.09E-06	0.00088	1.29 (626,6032,266)
GO:0006399	tRNA metabolic process	3.62E-06	0.00148	1.90 (180,3004,56)
GO:0022904	respiratory electron transport chain	5.96E-06	0.00237	1.81 (80,6313,50)
GO:0006612	protein targeting to membrane	6.21E-06	0.00241	1.58 (152,5869,77)
GO:0065003	protein-containing complex assembly	7.47E-06	0.00283	1.17 (1500,6334,606)
GO:0006807	nitrogen compound metabolic process	1.21E-05	0.00446	1.07 (6618,6326,2437)
GO:0006120	mitochondrial electron transport, NADH to ubiquinone	1.28E-05	0.00461	2.41 (38,4999,25)
GO:0022607	cellular component assembly	1.40E-05	0.00496	1.16 (2315,4823,706)
GO:0022618	ribonucleoprotein complex assembly	1.83E-05	0.00632	1.49 (215,5494,96)
GO:0071826	ribonucleoprotein complex subunit organization	1.92E-05	0.00649	1.46 (229,5689,104)
GO:0072594	establishment of protein localization to organelle	2.27E-05	0.00750	1.62 (377,2588,86)
GO:0071704	organic substance metabolic process	2.38E-05	0.00770	1.06 (7450,6318,2720)
GO:0006418	tRNA aminoacylation for protein translation	3.65E-05	0.01160	2.42 (45,4207,25)
GO:0043039	tRNA aminoacylation	4.35E-05	0.01350	2.36 (48,4207,26)
GO:0006457	protein folding	4.60E-05	0.01400	1.49 (205,5263,88)
GO:0006605	protein targeting	5.29E-05	0.01580	1.65 (310,2574,72)
GO:0002181	cytoplasmic translation	5.31E-05	0.01560	2.54 (39,4066,22)
GO:2000143	negative regulation of DNA-templated transcription, initiation	5.35E-05	0.01540	22.13 (6,552,4)
GO:0044267	cellular protein metabolic process	5.97E-05	0.01690	1.14 (3250,3849,779)
GO:0008152	metabolic process	6.03E-05	0.01670	1.05 (7940,6318,2884)
GO:0043038	amino acid activation	7.16E-05	0.01950	2.31 (49,4207,26)
GO:0044265	cellular macromolecule catabolic process	7.61E-05	0.02040	1.27 (776,4739,254)
GO:0006414	translational elongation	8.00E-05	0.02110	1.60 (117,6249,64)
GO:0034250	positive regulation of cellular amide metabolic process	8.94E-05	0.02310	1.82 (137,3314,45)
GO:1903047	mitotic cell cycle process	0.00011	0.02910	1.67 (561,1392,71)
GO:0044238	primary metabolic process	0.00012	0.02890	1.06 (7089,6312,2581)
GO:0033365	protein localization to organelle	0.00015	0.03580	1.36 (622,3356,155)
GO:0070125	mitochondrial translational elongation	0.00019	0.04520	1.67 (88,6247,50)
GO:1900193	regulation of oocyte maturation	0.00019	0.04590	6.39 (7,2459,6)
GO:0008535	respiratory chain complex IV assembly	0.00019	0.04540	2.53 (24,5140,17)
GO:0000083	regulation of transcription involved in G1/S transition of mitotic cell cycle	0.00020	0.04460	15.43 (28,212,5)
GO:0051276	chromosome organization	0.00020	0.04510	1.33 (379,5347,147)
GO:0036295	cellular response to increased oxygen levels	0.00022	0.04860	6.81 (14,1346,7)

[a] GO IDs with an FDR (false discovery rate) < 0.05 are listed. 'B' is the total number of genes associated with a specific GO term; 'n' is the number of genes in the target set; 'b' is the number of genes in the intersection; there are a total of 18323 GO genes at the time of analysis; enrichment = (b/n)/(B/18323).

Supplementary Table S8. Top disrupted biological processes negatively selected by cisplatin in A375 cells[a].

GO id	GO term	p-value	FDR	Enrichment (B, n, b)
GO:0043161	proteasome-mediated ubiquitin-dependent protein catabolic process	2.21E-07	0.0034	12.59 (291,45,9)
GO:0010498	proteasomal protein catabolic process	4.05E-07	0.0031	11.75 (312,45,9)
GO:0006511	ubiquitin-dependent protein catabolic process	1.39E-06	0.0072	8.64 (471,45,10)
GO:1903827	regulation of cellular protein localization	1.47E-06	0.0057	8.63 (494,43,10)
GO:0019941	modification-dependent protein catabolic process	1.54E-06	0.0048	8.54 (477,45,10)
GO:0043632	modification-dependent macromolecule catabolic process	1.90E-06	0.0049	8.36 (487,45,10)
GO:0048523	negative regulation of cellular process	2.58E-06	0.0057	3.15 (4547,23,18)
GO:0032446	protein modification by small protein conjugation	3.20E-06	0.0062	23.49 (650,6,5)
GO:0031330	negative regulation of cellular catabolic process	3.82E-06	0.0066	13.83 (244,38,7)
GO:0060019	radial glial cell differentiation	3.86E-06	0.0060	61.08 (12,100,4)

GO:0032268	regulation of cellular protein metabolic process	3.96E-06	0.0056	3.39 (2516,43,20)
GO:0030163	protein catabolic process	4.38E-06	0.0057	8.96 (409,45,9)
GO:0031146	SCF-dependent proteasomal ubiquitin-dependent protein catabolic process	4.62E-06	0.0055	208.22 (44,6,3)
GO:0051603	proteolysis involved in cellular protein catabolic process	5.20E-06	0.0058	7.55 (539,45,10)
GO:0009895	negative regulation of catabolic process	1.12E-05	0.0116	11.76 (287,38,7)
GO:0051246	regulation of protein metabolic process	1.16E-05	0.0113	3.16 (2700,43,20)
GO:0045116	protein neddylation	1.40E-05	0.0128	939.64 (13,3,2)
GO:0032270	positive regulation of cellular protein metabolic process	1.43E-05	0.0123	4.17 (1533,43,15)
GO:0043687	post-translational protein modification	1.56E-05	0.0128	34.12 (358,6,4)
GO:0031399	regulation of protein modification process	1.59E-05	0.0124	3.87 (1761,43,16)
GO:0070647	protein modification by small protein conjugation or removal	1.61E-05	0.0119	17.14 (891,6,5)
GO:0044265	cellular macromolecule catabolic process	1.97E-05	0.0139	5.77 (776,45,11)
GO:0048519	negative regulation of biological process	2.25E-05	0.0152	1.96 (5268,71,40)
GO:0019538	protein metabolic process	2.87E-05	0.0186	2.36 (3946,55,28)
GO:0051247	positive regulation of protein metabolic process	2.95E-05	0.0183	3.93 (1628,43,15)
GO:0031396	regulation of protein ubiquitination	2.98E-05	0.0178	10.13 (189,67,7)
GO:0044267	cellular protein metabolic process	3.47E-05	0.0199	2.56 (3250,55,25)
GO:0031329	regulation of cellular catabolic process	3.59E-05	0.0199	4.63 (768,67,13)
GO:2000737	negative regulation of stem cell differentiation	4.41E-05	0.0236	36.65 (20,100,4)
GO:0044260	cellular macromolecule metabolic process	4.43E-05	0.0229	1.90 (4559,93,44)
GO:0051726	regulation of cell cycle	4.57E-05	0.0229	6.44 (1114,23,9)
GO:0006464	cellular protein modification process	5.28E-05	0.0256	2.37 (2915,77,29)
GO:0036211	protein modification process	5.28E-05	0.0249	2.37 (2915,77,29)
GO:2000978	negative regulation of forebrain neuron differentiation	5.90E-05	0.0269	183.23 (2,100,2)
GO:1901658	glycosyl compound catabolic process	6.51E-05	0.0289	2.08 (42,5875,28)
GO:1903320	regulation of protein modification by small protein conjugation or removal	6.70E-05	0.0289	8.90 (215,67,7)
GO:0042509	regulation of tyrosine phosphorylation of STAT protein	8.10E-05	0.0340	14.09 (78,100,6)
GO:0032880	regulation of protein localization	8.73E-05	0.0357	4.98 (942,43,11)
GO:0009057	macromolecule catabolic process	0.00012	0.0482	4.79 (935,45,11)
GO:0042127	regulation of cell proliferation	0.00013	0.0511	2.82 (1588,86,21)
GO:0009894	regulation of catabolic process	0.00013	0.0507	5.21 (879,40,10)
GO:0072102	glomerulus morphogenesis	0.00013	0.0495	24.43 (3,750,3)
GO:0070757	interleukin-35-mediated signaling pathway	0.00013	0.0485	13.39 (11,622,5)
GO:0070106	interleukin-27-mediated signaling pathway	0.00014	0.0484	56.15 (11,89,3)
GO:0016567	protein ubiquitination	0.00014	0.0490	20.29 (602,6,4)

[a] GO IDs with an FDR (false discovery rate) < 0.05 are listed. 'B' is the total number of genes associated with a specific GO term; 'n' is the number of genes in the target set; 'b' is the number of genes in the intersection; there are a total of 18323 GO genes at the time of analysis; enrichment = (b/n)/(B/18323).

Supplementary Table S9. Negative selection of disrupted DNA repair pathways by cisplatin in A375 cells.

GO term	Gene[a]	p-value	FDR	Rank[b]	Good sgRNA
DNA repair	455	0.0272	0.2831	360	125
nucleotide excision repair	112	0.0388	0.3203	448	38
transcription coupled nucleotide excision repair	72	0.0431	0.3321	523	26
postreplication repair	53	0.0481	0.3478	599	14
global genome nucleotide excision repair	32	0.1009	0.4341	1077	13
non recombinational repair	69	0.3491	0.6754	2087	22
mismatch repair	27	0.5270	0.7746	3018	6
base excision repair	38	0.6100	0.8163	3210	7
double strand break repair	156	0.7077	0.8588	3246	39
interstrand cross link repair	42	0.7653	0.8854	3708	8
recombinational repair	71	0.9749	0.9858	4287	13

[a] Total number of genes associated with a specific GO biological process term. [b] The rank is among all the 4437 GO biological processes (including all parent and child processes).